

Learning to Partially Defer for Sequences

Anonymous authors

Paper under double-blind review

Abstract

In the Learning to Defer (L2D) framework, a prediction model can either make a prediction or defer it to an expert, as determined by a rejector. Current L2D methods train the rejector to decide whether to reject the *entire prediction*, which is not desirable when the model predicts long sequences. We present an L2D setting for sequence outputs where the system can defer *specific outputs* of the whole model prediction to an expert in an effort to interleave the expert and machine throughout the prediction. We propose two types of model-based post-hoc rejectors for pre-trained predictors: a token-level rejector, which defers specific token predictions to experts with next token prediction capabilities, and a one-time rejector for experts without such abilities, which defers the remaining sequence from a specific point onward. In the experiments, we also empirically demonstrate that such granular deferrals achieve better cost-accuracy tradeoffs than whole deferrals on Traveling salesman solvers, News summarization, and Weather prediction.

1 Introduction

Trustworthiness of AI is under scrutiny with its increased deployment in highly consequential areas like healthcare (Ker et al., 2017; Courtiol et al., 2019; Asan et al., 2020) and criminal justice (Dressel & Farid, 2018; Rigano, 2019; Alikhademi et al., 2022). Hybrid intelligent systems (Kamar, 2016; Dellermann et al., 2019; Akata et al., 2020; Maadi et al., 2021) approach this problem through collaborations between either humans and machines or two machines to improve confidence in the system. Specifically, Learning to Defer (L2D) (Madras et al., 2018) accommodates these teams by allowing the model to defer to an expert when it is uncertain about a prediction task with the objective of maximizing overall system accuracy while minimizing deferral costs.

Existing L2D methods focus on multiclass (Mozannar & Sontag, 2020; Cao et al., 2022; Verma & Nalisnick, 2022; Mao et al., 2024a;c) and scalar regression (Cheng et al., 2024; Mao et al., 2024b) problems. However, these methods only support complete deferral of predictions, resulting in costs that scale with the output size, when applied to large *sequence outputs* (Narasimhan et al., 2024). This is inefficient if only parts of the model’s prediction are inaccurate. The prevalence of sequences in areas such as drug discovery (Wang et al., 2018; Jumper et al., 2021; Dauparas et al., 2022; Nijkamp et al., 2023) and language modeling (Kenton & Toutanova, 2019; Brown et al., 2020; Raffel et al., 2020) calls for a cost-effective extension of the L2D framework to handle sequential outputs.

To this end, we propose a fine-grained approach to deferral where the system has the flexibility to defer *portions* of the predicted sequence. For example, in part of speech tagging, this mechanism would only require the expert to tag a few uncertain sentences in a paragraph rather than the whole paragraph, reducing the time cost which increases with the number of words to be tagged. This can, therefore, achieve a more favorable cost-accuracy tradeoff, which can further improve as the deferrals become more precise - for example, at the word-level. Additionally, parts of the prediction task completed by the predictor can also function as contextual clues for the language expert to fill in the deferred parts, further minimizing deferral costs.

While partial deferral is therefore desirable, the granularity of such deferrals depends on the size of the sequence segments the expert can predict at a time. For instance, if the expert is a next-token predictor, it can complete spans as small as a single token—*token-level* deferral. This is especially valuable when

the model’s predictive quality across all parts of the output are dependent. Specifically, in autoregressive prediction, uncertainty at earlier prediction points can propagate and degrade later points (Bengio et al., 2015; Lamb et al., 2016; Schmidt, 2019). Thus, to achieve a better cost-accuracy tradeoff, the token-level rejector can orchestrate a dynamic collaboration between the predictor and the expert where the predictor receives an expert prediction on an early substructure before the model veers “off-course”.

This, however, is only feasible with experts that can make predictions one token at a time. That said, partial deferrals can still be implemented as long as the expert is at least capable of completing the predicted sequence given a partial subsequence from the model. We refer to this type of deferral as *one-time* deferral. For example, Gurobi solvers for Traveling salesman problems lack the ability to iteratively select the next city in the tour, but they can use partial subtours generated by models as constraints to generate the entire tour at a reduced cost. In this case, the one-time rejector would select a point in the sequence from which the expert completes the sequence.

In this paper, we make the following contributions:

- We present a novel L2D framework where the rejector interweaves the expert’s and machine’s predictions to improve cost-accuracy tradeoffs. We divide this setting into token-level and one-time deferrals based on the granularity of the deferrals, thereby accommodating various types of experts.
- We propose convex surrogate losses that offer Bayes consistency guarantees leading to implementable model-based post hoc rejectors for pre-trained predictors for each type of deferral. We further analyze the surrogates theoretically through generalization bounds.
- We empirically demonstrate improved cost-accuracy tradeoffs when using model-based rejectors for either deferrals against whole sequence rejectors with Traveling salesman solvers, News summarization, and Weather prediction.

2 Background

2.1 Learning to Defer

Deferrals, also known as rejections or abstentions, are classified into two types - *confidence*-based (Chow, 1957; Bartlett & Wegkamp, 2008; Yuan & Wegkamp, 2010; Ramaswamy et al., 2018) and *model*-based (Cortes et al., 2016; Madras et al., 2018; Mozannar & Sontag, 2020; Verma & Nalisnick, 2022; Cao et al., 2022; Mao et al., 2024a; Cheng et al., 2024; Mao et al., 2024b). *Confidence*-based methods learn a predictor that outputs confidences; a prediction is rejected whenever its confidence falls below a cost-dependent threshold. However, Madras et al. (2018) and Cortes et al. (2016) characterized the suboptimality of these methods and advocated for the rejector to be a model trained either simultaneously with the predictor or post-hoc: this is the *model*-based approach. This system seeks to minimize the following loss function:

$$\mathcal{L}_{\text{L2D}}(h, r, e, x, y) = l(y, h(x))\mathbf{1}_{r(x)<0} + c(x, y, e)\mathbf{1}_{r(x)\geq 0} \quad (1)$$

where h is the predictor, r is the rejector, e is the expert, $l(y, h(x))$ is the model loss, and $c(x, y, e)$ is the cost incurred when deferring to an expert.

Although our setting assumes access to a single expert, one-time deferral closely resembles L2D with multiple experts (Verma et al., 2023; Mao et al., 2024b). We formalize this similarity and its implications in Section 4.1. For E experts, L2D minimizes:

$$\mathcal{L}_{\text{L2DMulti}}(h, r, x, y, \{e_j\}_{j=1}^E) = l(y, h(x))\mathbf{1}_{r(x)=0} + \sum_{j=1}^E c_j(x, y, e_j)\mathbf{1}_{r(x)=j} \quad (2)$$

where $c_j(x, y, e_j)$ is the cost of querying the j^{th} expert, e_j . The rejector must decide which expert to defer to.

2.2 Consistent Losses

Direct minimization of Equations (1) and (2) is challenging due to the non-convexity and discontinuities. This can be addressed by optimizing a convex surrogate loss function which, upon minimization, will lead to the same outcome as minimizing the original loss. This property is formally called *Bayes Consistency*.

Definition 2.1 (Consistency). Let the risk of a hypothesis f with respect to a loss l be $\mathcal{R}_l(f) = \mathbb{E}_{(x,y) \sim \mathcal{P}_{\mathcal{X},\mathcal{Y}}}[l(f(x), y)]$. Let the optimal risk with respect to l out of all hypotheses in \mathcal{F} be $\mathcal{R}_l^*(\mathcal{F}) = \inf_{f \in \mathcal{F}} \mathcal{R}_l(f)$. A surrogate loss function, $\phi(\cdot)$, is said to be \mathcal{F} -consistent with respect to l if for any $f_n \in \mathcal{F}$, the following property holds true:

$$\lim_{n \rightarrow \infty} \mathcal{R}_\phi(f_n) - \mathcal{R}_\phi^*(\mathcal{F}) = 0 \Rightarrow \lim_{n \rightarrow \infty} \mathcal{R}_l(f_n) - \mathcal{R}_l^*(\mathcal{F}) = 0$$

When \mathcal{F} is the class of all measurable functions, a surrogate ϕ is Bayes consistent for a target loss l if there exists a nondecreasing function $\Gamma : \mathbb{R} \rightarrow \mathbb{R}$ continuous at 0 with $\Gamma(0) = 0$, such that for all f ,

$$\mathcal{R}_l(f) - \mathcal{R}_l^* \leq \Gamma(\mathcal{R}_\phi(f) - \mathcal{R}_\phi^*)$$

where $\mathcal{R}_l^* = \inf_f \mathcal{R}_l(f)$ is the optimal risk over all measurable functions. We introduce surrogates for both token-level and one-time deferral (similar to Equations (1) and (2)) and prove they satisfy the above inequality, thereby establishing Bayes consistency.

3 Token-level partial deferral

Let $\mathcal{Y} \subseteq \bigcup_{\ell=1}^L \mathcal{V}^\ell$ denote the space of sequences over label set \mathcal{V} with maximum length L . For $y \in \mathcal{Y}$, the j^{th} token is $y_j \in \mathcal{V}$. \mathcal{V} can be a finite vocabulary in the case of text sequences and be \mathbb{R} when the output is a scalar time series. Let \mathcal{X} be the feature space. In sequence generation, $\mathcal{X} \subseteq \mathbb{R}^d$ would be a d -dimensional feature space, whereas $\mathcal{X} = \mathcal{V}^{L'}$ would be a sequence space in sequence-to-sequence learning. Let $\mathcal{P}_{\mathcal{X},\mathcal{Y}}$ denote the data-generating distribution over $\mathcal{X} \times \mathcal{Y}$.

Suppose we have a predictor h and a stronger expert e . e takes in $x \in \mathcal{X}$ and the leftward context $\hat{y}_{<j} = (\hat{y}_1, \dots, \hat{y}_{j-1}) \in \mathcal{V}^{j-1}$ to predict y_j ; repeated calls can auto-regressively complete the sequence. e can, for instance, be a human or a large autoregressive model. However, querying e is more expensive than calls to h . We, therefore, wish to design an L2D system where experts can complete uncertain tokens in the model's prediction, facilitating more fine-grained deferrals – referred to as *token-level* deferrals – yielding a more favorable cost-quality tradeoff than deferring the entire sequence.

If h is autoregressive, token-level deferrals allows h to leverage the expert-supplied tokens when generating subsequent tokens, enabling a seamless and adaptive collaboration. This mitigates uncertainty propagation, reduces the number of expert queries, and improves cost-effectiveness. While this paradigm can apply to all sequence predictors, we will specifically focus on a dynamic L2D system with an autoregressive predictor.

In this setting, at step j , the rejector r_j takes in $(x, \hat{y}_{<j})$ where $\hat{y}_{<j}$ may mix predictor and expert tokens. When $r_j(x, \hat{y}_{<j}) \geq 0$, it rejects the j^{th} label prediction from h and receives an expert prediction \hat{y}_j^e . Otherwise, the model will keep the prediction from h , i.e. $\hat{y}_j^h = h(x, \hat{y}_{<j})$. For a fixed h and a specific instance of $(x, \hat{y}_{<j}, y)$, r_j is trained to minimize:

$$\mathcal{L}_j(h, r_j, x, \hat{y}_{<j}, y) = l(y, \hat{y}_j^h) \mathbf{1}_{r_j(x, \hat{y}_{<j}) < 0} + c_j(x, \hat{y}_{<j}, y) \mathbf{1}_{r_j(x, \hat{y}_{<j}) \geq 0} \quad (3)$$

where $l(y, \hat{y}_j^h)$ is the loss from using \hat{y}_j^h and $c_j(x, \hat{y}_{<j}, y)$ is the deferral cost. $l(y, \hat{y}_j^h)$ can be the mean squared error defined by $(y_j - \hat{y}_j^h)^2$ or a 0-1 loss between the true j^{th} token and \hat{y}_j^h in text sequences. Generally, $l(y, \hat{y}_j^h)$ can be viewed as token-level feedback to generate an accurate complete sequence. $c_j(x, \hat{y}_{<j}, y)$ can be a constant c_j to reflect expert query costs but it can also be $l(y, \hat{y}_j^e)$ to account for the expert's errors.

Finally, the predicted j^{th} label $\hat{y}_j = \hat{y}_j^h \mathbf{1}_{r_j(x, \hat{y}_{<j}) < 0} + \hat{y}_j^e \mathbf{1}_{r_j(x, \hat{y}_{<j}) \geq 0}$ is appended to $\hat{y}_{<j}$ to serve as input for $(j+1)^{\text{th}}$ token prediction, and this continues until L labels are generated. The total loss for the sequence

is $\mathcal{L}^{\text{Token}}(h, r, x, y) = \frac{1}{L} \sum_{j=1}^L \mathcal{L}_j(h, r_j, x, \hat{y}_{<j}, y)$ where $r = [r_1 \ \dots \ r_L]^T$. The $\mathcal{L}^{\text{Token}}$ -risk is denoted by $\mathcal{R}_{\text{Token}}(h, r) = \mathbb{E}_{(x,y) \sim \mathcal{P}_{X,Y}}[\mathcal{L}^{\text{Token}}(h, r, x, y)]$.

For analysis, we assume teacher-forced training (Williams & Zipser, 1989; Lamb et al., 2016): at j^{th} step, \mathcal{L}_j is evaluated on the output of r_j , but we roll out the leftward context for step $j+1$ using the oracle rejection decision $\mathbf{1}_{l(y, \hat{y}_j^h) \geq c_j(x, \hat{y}_{<j}, y)}$. This decouples the training distribution of $\hat{y}_{<j}$ from the router’s predictions; the context depends only on (x, y) via the predictor and expert outputs. In experiments, we don’t limit ourselves to teacher forcing training due to the risk of exposure bias; see Appendix H.

3.1 Surrogate Loss

As described in Section 2.2, minimizing the deferral loss directly is computationally difficult, so identifying an optimal rejector requires optimizing a convex surrogate loss that is Bayes consistent with respect to $\mathcal{L}^{\text{Token}}$. To this end, we propose the following surrogate loss function: $\mathcal{L}^\phi(h, r, x, y) = \frac{1}{L} \sum_{j=1}^L \mathcal{L}_j^\phi(h, r_j, x, \hat{y}_{<j}, y)$ where

$$\mathcal{L}_j^\phi(h, r_j, x, \hat{y}_{<j}, y) = l(y, \hat{y}_j^h) \phi(r_j(x, \hat{y}_{<j})) + c_j(x, \hat{y}_{<j}, y) \phi(-r_j(x, \hat{y}_{<j})) \quad (4)$$

and ϕ is a convex binary surrogate loss. ϕ could, for example, be the logistic loss, i.e., $\phi(z) = \log(1 + \exp\{-z\})$, or the square loss, i.e., $\phi(z) = (1 - z)^2$. \mathcal{L}^ϕ -risk is characterized by $\mathcal{R}_\phi(h, r) = \mathbb{E}_{(x,y) \sim \mathcal{P}_{X,Y}}[\mathcal{L}^\phi(h, r, x, y)]$.

The optimization of $\mathcal{L}^\phi(h, r, x, y)$ is feasible due its convexity. Additionally, it upper bounds $\mathcal{L}^{\text{Token}}$ upto a scaling factor, providing alignment between reducing the surrogate loss and reducing the desired loss function. The proof of these properties can be found in Appendix A.1.

To show Bayes consistency of the surrogate, we relate the excess risk using $\mathcal{L}^{\text{Token}}$ and the excess risk using \mathcal{L}^ϕ in Lemma 3.1. The proof employs a specific type of distribution on $\mathcal{X} \times \{-1, 1\}$ with mass on functions of the conditional expectations of $l(y, \hat{y}_j^h)$ and $c_j(x, \hat{y}_{<j}, y)$ to relate the two inequalities - a strategy inspired by Mao et al. (2024a). The complete proof can be found in Appendix A.2.

Lemma 3.1. *Let $0 < \bar{c} \leq c_j(x, \hat{y}_{<j}, y) \leq \bar{C} < \infty$ for all j , $0 \leq l(y, \hat{y}_j^h) \leq \bar{l} < \infty$, and ϕ be a binary surrogate loss that satisfies the following inequality for any distribution over $\mathcal{X} \times \{-1, 1\}$ and any measurable function f :*

$$\mathcal{R}_{\text{binary } 0-1}(f) - \mathcal{R}_{\text{binary } 0-1}^*(f) \leq \Gamma(\mathcal{R}_{\text{binary } \phi}(f) - \mathcal{R}_{\text{binary } \phi}^*(f))$$

where $\mathcal{R}_{\text{binary } 0-1}$ is the binary 0-1 risk and $\Gamma: \mathbb{R}^+ \rightarrow \mathbb{R}^+$ is a non-decreasing concave function. Then, for any measurable r and any h , the following inequality holds for any distribution over $\mathcal{X} \times \mathcal{Y}$:

$$\mathcal{R}_{\text{Token}}(r, h) - \mathcal{R}_{\text{Token}}^*(h) \leq \tilde{\Gamma}(\mathcal{R}_\phi(r, h) - \mathcal{R}_\phi^*(h))$$

where $\tilde{\Gamma}(z) = (\bar{l} + \bar{C}) \Gamma(\frac{z}{\bar{l}})$, $\mathcal{R}_{\text{Token}}^*(h) := \inf_r \mathcal{R}_{\text{Token}}(r, h)$, and $\mathcal{R}_\phi^*(h) := \inf_r \mathcal{R}_\phi(r, h)$

Taking the limit on both sides of the inequality result of Lemma 3.1 proves consistency of the surrogate loss, formally stated in Theorem 3.2. The proof of Theorem 3.2 hinges on the fact that a classification-calibrated surrogate loss satisfies the condition presented in Lemma 3.1. A loss ϕ is considered binary classification calibrated if the minimizer of the pointwise ϕ -risk or $\mathbb{E}_{y \sim \mathcal{P}_{Y|X=x}}[\phi(yf(x))]$ always has the same sign as $\mathbb{P}[Y = 1 | X = x] - \frac{1}{2}$. We defer the full proof of Theorem 3.2 and the formal definition of classification calibrated loss to Appendix A.3.

Theorem 3.2 (Consistency). *If $0 < \bar{c} \leq c_j(x, \hat{y}_{<j}, y) \leq \bar{C} < \infty$ for all j , $0 \leq l(y, \hat{y}_j^h) \leq \bar{l} < \infty$, and ϕ be binary classification calibrated, then, for a fixed h , \mathcal{L}^ϕ is a Bayes consistent surrogate for $\mathcal{L}^{\text{Token}}$.*

3.2 Generalization Bounds

While Bayes consistency is desirable, the property only holds in the limit of infinite data and does not possess finite sample guarantees. In practice, finding a risk minimizer over the entire class of measurable functions is extremely challenging, particularly because $\mathcal{P}_{X,Y}$ is usually unknown. With access to a rejector training

data set \mathcal{D} with n samples, we can only learn the optimal $\hat{r}_n \in \arg \min_{r \in \mathcal{F}} \hat{\mathcal{R}}_\phi(r)$ from a restricted hypothesis class \mathcal{F} by minimizing the empirical risk with respect to $\mathcal{L}^\phi - \hat{\mathcal{R}}_\phi(r) = \frac{1}{n} \sum_{(x^i, y^i) \in \mathcal{D}} \mathcal{L}^\phi(h, r, x^i, y^i)$. We now present an upper bound for the estimation error to characterize the quality of \hat{r}_n with respect to \mathcal{F} . Please refer to Appendix A.4 for the full proof.

Theorem 3.3. *Suppose $r \in \mathcal{F}$ which is composed of $\{\mathcal{F}_j\}_{j=1}^L$ such that $r_j \in \mathcal{F}_j$, $c_j(x) \leq \bar{C}$, and $l(y, \hat{y}_j^h) \leq \bar{l}$. If ϕ is ρ -lipschitz continuous, then with probability $1 - \delta$, the following upper bound holds for the empirical risk minimizer \hat{r}_n with respect to \mathcal{L}_ϕ :*

$$\mathcal{R}_\phi(\hat{r}_n) - \mathcal{R}_\phi^*(\mathcal{F}) \leq \frac{4\rho\sqrt{2(\bar{C}^2 + \bar{l}^2)}}{L} \sum_{j=1}^L \mathfrak{R}_n(\mathcal{F}_j) + (\bar{C} + \bar{l})\sqrt{\frac{2\log(\frac{2}{\delta})}{n}}$$

where $\mathcal{R}_\phi^*(\mathcal{F}) = \inf_{r \in \mathcal{F}} \mathcal{R}_\phi(r)$ and $\mathfrak{R}_n(\mathcal{F}_j)$ is the Rademacher Complexity of \mathcal{F}_j

From Theorem 3.3, the estimation error of using \hat{r}_n with respect to \mathcal{L}^ϕ depends on the Rademacher complexity $\mathfrak{R}_n(\mathcal{F})$ of the hypothesis class. Theorem 3.3 alone does not describe the excess risk with respect to the original token loss $\mathcal{L}^{\text{Token}}$. Using Lemma 3.1, we express the upper bound of the excess risk in Corollary 3.4, and the proof can be found in Appendix A.5.

Corollary 3.4. *Suppose $r \in \mathcal{F}$ which is composed of $\{\mathcal{F}_j\}_{j=1}^L$ such that $r_j \in \mathcal{F}_j$, $0 < \bar{c} \leq c_j(x) \leq \bar{C}$, and $l(y, \hat{y}_j^h) \leq \bar{l} < \infty$. If ϕ is a ρ -lipschitz continuous binary classification-calibrated function, then with probability $1 - \delta$, the following upper bound on the excess risk with respect to $\mathcal{L}^{\text{Token}}$ holds for the empirical risk minimizer \hat{r}_n with respect to \mathcal{L}_ϕ for a fixed h :*

$$\mathcal{R}_{\text{Token}}(\hat{r}_n, h) - \mathcal{R}_{\text{Token}}^*(h) \leq \tilde{\Gamma}(\mathcal{B}(\mathcal{F}) + \mathcal{A}_\phi(\mathcal{F}, h))$$

where $\tilde{\Gamma}$ is a non-decreasing function, $\mathcal{B}(\mathcal{F}) = \frac{4\rho\sqrt{2(\bar{C}^2 + \bar{l}^2)}}{L} \sum_{j=1}^L \mathfrak{R}_n(\mathcal{F}_j) + (\bar{C} + \bar{l})\sqrt{\frac{2\log(\frac{2}{\delta})}{n}}$, and $\mathcal{A}_\phi(\mathcal{F}, h) = \mathcal{R}_\phi^*(\mathcal{F}, h) - \mathcal{R}_\phi^*(h)$ is the approximation error.

4 One-time partial deferral

Token-level deferrals are ideal to produce partial deferrals, but they hinge on the expert’s capability to perform next-token prediction instead of generating the entire sequence at once. If the expert is at least capable of completing sequences using predicted subsequences from models, the system can achieve better cost-quality tradeoffs with partial deferrals compared to whole deferrals, albeit constrained by the lack of granularity in deferral, through *one-time* deferral. In the one-time partial deferral setting, the rejector takes in x as input and identifies a point in sequence - referred to as the *deferral point* - from which the expert predicts the remaining sequence. When $r(x) = j$, the rejector chooses to reject the prediction of the sequence from the j^{th} token onward and thereafter defers to the expert. In doing so, the system incurs a loss of $l(y, \hat{y}_{<j})$ for using the first j tokens from the predictor h and pays a cost of $\tilde{c}_j(x, \hat{y}_{<j}, y)$ for using the expert with the partial feedback from h . When $r(x) = 1$, the entire prediction task is deferred to the expert. If $r(x) = L + 1$, the model completes the full prediction without paying any cost for an expert. For this deferral point classification, our objective is to minimize the following loss function:

$$\mathcal{L}_{\text{Full}}^{\text{OneTime}}(h, r, x, y) = \sum_{j=1}^{L+1} (l(y, \hat{y}_{<j}) + \tilde{c}_j(x, \hat{y}_{<j}, y)) \mathbf{1}_{r(x)=j} \quad (5)$$

where $l(y, \hat{y}_{<1}) = 0$

4.1 Influence of large L

This paradigm closely parallels learning to defer with multiple experts as their objectives are analogous (Equations (2) and (5)). Each position j can be viewed as an “expert” whose prediction concatenates the model prefix $\hat{y}_{<j}$ with the expert-completed suffix $\hat{y}_{\geq j}^e$. Prior work shows diminishing accuracy gains as the

number of experts increases, which can reduce cost-effectiveness (Verma et al., 2023; Hemmer et al., 2023). This suggests that allowing deferral at every position may be over-resolved, since adjacent deferral points can yield similar accuracy.

Towards this end, we wish to allow for flexibility in adjusting the number of “experts”. We achieve this by considering a generalization of one-time deferral where the predictor can defer to the expert on a select set of token positions specified by \mathcal{J} , instead of having all token positions be potential deferral points. For this generalization, we consider the following loss:

$$\mathcal{L}^{\text{OneTime}}(h, r, x, y) = \sum_{j \in \mathcal{J}} (l(y, \hat{y}_{<j}) + \tilde{c}_j(x, \hat{y}_{<j}, y)) \mathbf{1}_{r(x)=j} \quad (6)$$

The $\mathcal{L}^{\text{OneTime}}$ -risk is denoted by $\mathcal{R}^{\text{OneTime}}(h, r) = \mathbb{E}_{(x,y) \sim \mathcal{P}_{X,Y}}[\mathcal{L}^{\text{OneTime}}(h, r, x, y)]$.

4.2 Surrogate loss

Let \mathbf{g} consist of $|\mathcal{J}|$ scoring functions $g_j : \mathcal{X} \rightarrow \mathbb{R}$ where j indexes the token positions in a sequence and let $r(x) = \arg \max_{j \in \mathcal{J}} g_j(x)$. We propose the following surrogate loss function:

$$\mathcal{L}^\psi(h, r, x, y) = \sum_{j \in \mathcal{J}} (c_{\max} - l(y, \hat{y}_{<j}) - \tilde{c}_j(x, \hat{y}_{<j}, y)) \psi(\mathbf{g}(x), j)$$

where $\psi(\mathbf{g}(x), j)$ is a consistent surrogate for the multiclass 0-1 loss or $\mathbf{1}_{r(x) \neq j}$, and $c_{\max} = \max_{j \in \mathcal{J}} l(y, \hat{y}_{\leq j}) + \tilde{c}_j(x, \hat{y}_{<j}, y)$. Examples of ψ include cross entropy loss, i.e. $\psi_{\text{ce}}(\mathbf{g}(x), j) = -\log \frac{e^{g_j(x)}}{\sum_{k \in \mathcal{J}} e^{g_k(x)}}$ or mean absolute error, i.e. $\psi_{\text{mae}}(\mathbf{g}(x), j) = 1 - \frac{e^{g_j(x)}}{\sum_{k \in \mathcal{J}} e^{g_k(x)}}$ (Ghosh et al., 2017). The \mathcal{L}^ψ -risk is characterized by $\mathcal{R}_\psi(h, r) = \mathbb{E}_{(x,y) \sim \mathcal{P}_{X,Y}}[\mathcal{L}^\psi(h, r, x, y)]$.

Intuitively, for a given token position j , $c_{\max} - l(y, \hat{y}_{\leq j}) - \tilde{c}_j(x, \hat{y}_{<j}, y)$ is large when the subsequence up till j can be predicted correctly and the cost of deferring on the rest of the sequence is small. When this term is large, we desire $\psi(\mathbf{g}(x), j)$ to be small, incentivizing the model to choose j as the deferral point to minimize the surrogate loss. This surrogate loss encourages the rejector to pick a token position which also has minimal costs for deferring on the rest of the sequence - a goal the $\mathcal{L}^{\text{OneTime}}$ loss function shares.

Just like \mathcal{L}^ϕ , \mathcal{L}^ψ is also convex and upper bounds $\mathcal{L}^{\text{OneTime}}$ up to some scale γ (See Appendix B.2 for proof). Theorem 4.1 shows that \mathcal{L}^ψ achieves Bayes consistency.

Theorem 4.1 (Consistency). *Let $\tilde{c}_j(x, \hat{y}_{<j}, y) \leq \bar{C} < \infty$, $l(y, \hat{y}_j^h) \leq \bar{l} < \infty$ for all $j \in \mathcal{J}$, and ψ be cross entropy loss ψ_{ce} or mean absolute error ψ_{mae} . If there exists $i, j \in \mathcal{J}$ such that $|l(y, \hat{y}_i^h) + \tilde{c}_i(x, \hat{y}_{<i}, y) - l(y, \hat{y}_j^h) - \tilde{c}_j(x, \hat{y}_{<j}, y)| > \Delta > 0$, then, for a fixed h , \mathcal{L}^ψ is a consistent surrogate for $\mathcal{L}^{\text{OneTime}}$.*

The proof of the above theorem can be found in Appendix B.4. If the $l(y, \hat{y}_{\leq j}) + \tilde{c}_j(x, \hat{y}_{<j}, y)$ terms are equal for all j , the weights would be 0. By assuming a non-zero cost difference for at least one pair, we are ensuring that at least one j has a non-zero weight. Such an assumption can be satisfied if there is a sufficient separation in predictive capabilities between the predictor and the expert.

4.3 Generalization Bounds

Under the empirical risk minimization framework, the optimal rejector $\hat{r}_n \in \arg \min_{r \in \mathcal{F}} \hat{\mathcal{R}}_\psi(r)$ minimizes the empirical risk with respect to \mathcal{L}^ψ or $\hat{\mathcal{R}}_\psi(r) = \frac{1}{n} \sum_{(x^i, y^i) \in \mathcal{D}} \mathcal{L}^\psi(h, r, x^i, y^i)$ from a finite hypothesis class \mathcal{F} . Theorem 4.2 presents generalization bounds for \mathcal{L}^ψ (See Appendix B.5 for the proof).

Theorem 4.2. *Suppose $r_n \in \mathcal{F} = \{x \rightarrow \arg \min_{j \in \mathcal{J}} g_j(x) : g_j \in \mathcal{G}_j\}$ where \mathcal{G}_j consists of functions having a range of $(-M, M)$ with $M \geq 0$, $\tilde{c}_j(x, \hat{y}_{<j}, y) \leq \bar{C}$, and $l(y, \hat{y}_j^h) \leq \bar{l} < \infty$. If ψ is ρ -lipschitz continuous with respect to $\mathbf{g}(x)$ and there exists $u_\psi(M)$ such that $\psi(\mathbf{g}(x), j) \leq u_\psi(M) < \infty$ for all j and $r \in \mathcal{F}$, then*

with probability $1 - \delta$ for a fixed h , the following upper bound holds for the empirical risk minimizer \hat{r}_n with respect to $\mathcal{L}_\psi^{\text{Point}}$:

$$\mathcal{R}_\psi(\hat{r}_n, h) - \mathcal{R}_\psi^*(\mathcal{F}, h) \leq 2\sqrt{2}q(L)\rho \sum_{j \in \mathcal{J}} \mathfrak{R}_n(\mathcal{G}_j) + u_\psi(M)q(L)\sqrt{\frac{2 \log(\frac{2}{\delta})}{n}}$$

where $\mathcal{R}_\psi^*(\mathcal{F}, h) = \inf_{r \in \mathcal{F}} \mathcal{R}_\psi(r, h)$, $q(L) = 2(|\mathcal{J}| - 1)(\bar{C} + \bar{l})$, and $\mathfrak{R}_n(\mathcal{G}_j)$ is the Rademacher Complexity of \mathcal{G}_j .

Restricting the hypothesis class to have a range $(-M, M)$ practically involves ReLU activation and softmax clipping to prevent the scores \mathbf{g} from approaching $-\infty$ or ∞ . For ψ_{ce} , we can expect $u_{\psi_{\text{ce}}}(M) = -\log \frac{e^{-M}}{e^{-M} + Le^M}$ and for ψ_{mae} , it is $u_{\psi_{\text{mae}}}(M) = 1 - \frac{e^{-M}}{e^{-M} + Le^M}$. We can further express the upper bound of the excess risk respect to the original token loss $\mathcal{L}^{\text{OneTime}}$. The characterization of the upper bound and the proof details can be found in Appendix B.6.

5 Related Works

Model Cascades (Viola & Jones, 2001) share similarities with the learning to defer framework. In cascades, an inference task is progressively handled by a series of models where easier tasks are completed by earlier models in the sequence and complex cases escalate to subsequent models. Similar to confidence-based L2D methods described in Section 2.1, cascading decisions are typically determined by a thresholding deferral rule (Yue et al., 2023). Some recent work on applying cascades to large language models (Gupta et al., 2024; Wang et al., 2024) has also explored modeling the cascade decision maker. However, model cascades, just like learning to defer methods, ultimately rely on a single model for each prediction. Our work extends cascades by introducing partial deferrals, allowing two models to collaborate on a prediction. Narasimhan et al. (2024) also proposes a token-level deferral rule, but their deferral rule compares the predictor’s confidence with expert’s confidence at every token position, which requires many expensive expert queries. Our work learns the expert costs at training time to avoid such expert queries unless the rejector calls for it.

Query Routing methods select a model that provide the highest quality prediction from an ensemble of models. Some query routing algorithms in large language models (Jiang et al., 2023; Chen et al., 2023) often require querying either a part or the entire model ensemble to determine the best generation. Some methods train query routing models using specially designed loss functions (Shnitzer et al., 2023; Lu et al., 2023; Ding et al., 2024); these loss functions, however, lack consistency guarantees. Our work not only presents surrogate losses with stronger statistical guarantees but also offers more granular routing decisions.

Many L2D methods draw inspiration from the *Cost-Sensitive learning* framework. In the example-dependent cost-sensitive setting, each feature x is paired with a cost vector. A cost-sensitive classifier must then learn to identify the index of the cost vector that minimizes the expected cost. Classifiers (Abe et al., 2004; Lin, 2015) are often trained with a weighted logistic loss or weighted cross entropy loss function, similar to $\mathcal{L}^{\text{Token}}$ and $\mathcal{L}^{\text{OneTime}}$. However, popular methods (Tu & Lin, 2010; Chung et al., 2015) use losses that are inconsistent with the original cost-sensitive loss.

Selective classification equips a predictor with an abstention option that trades coverage for accuracy. In the noise-free setting, El-Yaniv & Wiener (2010) formalizes the risk-coverage framework. Deep variants implement the selection function via post-hoc confidence thresholding (Geifman & El-Yaniv, 2017) or joint learning (Geifman & El-Yaniv, 2019). Similarly, *selective regression* extends the reject option to regression (Shah et al., 2022; Jiang et al., 2020; Zaoui et al., 2020). However, unlike learning to defer, these methods treat abstention as a terminal action with a fixed penalty and do not account for the downstream effects of abstention, e.g., accuracy of expert predictions.

6 Experiments

Our experiments are designed to evaluate two questions: (i) how partial deferral compares to whole-sequence deferral, and (ii) how our model-based approach compares to confidence-based partial deferral. To this

end, we consider three tasks (TSP, XSUM, MWP). We refer the reader to Appendix D for training and hyperparameter details of the model rejectors.

6.1 Tasks

Traveling Salesman Problem (TSP): TSP is a classic NP-Hard optimization problems which requires finding the shortest tour visiting all cities exactly once and returning to the start. Optimization-based solvers achieve near-optimality at high computational cost, while ML models are efficient but less accurate. This task highlights a natural collaboration point for partial deferral. We use a PointerNet predictor (Vinyals et al., 2015), trained on synthetic 50-city TSP graphs (coordinates drawn from a standard normal distribution), and a Gurobi solver as the expert. The expert takes the partial solution from the predictor as a constraint and completes the tour. Tours are evaluated by total distance. Since Gurobi does not operate autoregressively, token-level deferral is unsuitable here; instead, this is a prime use case for one-time deferral. The loss $l(y, \hat{y}_{<j})$ measures the distance of subtour $\hat{y}_{<j}$, while the expert cost $\tilde{c}_j(x, \hat{y}_{<j}, y)$ combines the distance of the expert-completed subtour $\hat{y}_{\geq j}^e$ with a deferral cost α_j , which increases monotonically in the number of rejected tokens (see Appendix F).

Extreme Summarization (XSUM). The predictor summarizes long articles in a few sentences using a `t5-small` model, and the expert is a stronger `t5-base` model; both are fine-tuned on XSUM (Narayan et al., 2018). We use T5 (encoder–decoder) models because they can condition on any target prefix $\hat{y}_{<j}$, enabling the expert to complete a partial sequence without exchanging hidden states. By contrast, decoder-only models require reconstructing cross-model KV caches at step j , which defeats the purpose of partial feedback. Summaries are limited to 20 tokens and evaluated with ROUGE-1. For token-level deferral, the predictor loss is $l(y, \hat{y}_j^h) = \mathbf{1}_{\hat{y}_j^h \notin y}$, while the expert cost is $c_j(x, \hat{y}_{<j}, y) = \mathbf{1}_{e(x, \hat{y}_{<j}) \notin y}$. For one-time deferral, we measure $1 - \text{ROUGE1}$ score of the expert continuation from step j , appended to $\hat{y}_{<j}$. The joint term $l(y, \hat{y}_{\leq j}) + \tilde{c}_j(x, \hat{y}_{<j}, y)$ is the sum of this error and the deferral cost α_j , as in the TSP case.

Multi-Step Weather Prediction (MWP): Given 2 hours of temperature history (12 observations at 10-minute intervals), the task is to predict the next hour ($L = 6$). The predictor is an LSTM trained on real data from the Max Planck Institute in Jena, Germany. The expert is a simulated human: ground-truth values perturbed with zero-mean Gaussian noise. For token-level deferral, the predictor loss is mean-squared error $l(y, \hat{y}_j^h) = (\hat{y}_j^h - y_j)^2$, and the expert cost is $c_j(x, \hat{y}_{<j}, y) = (e(x, \hat{y}_{<j}) - y_j)^2$. For one-time deferral, the loss is $l(y, \hat{y}_{<j}) = \|y_{<j} - \hat{y}_{<j}\|_2^2$ and $\tilde{c}_j(x, \hat{y}_{<j}, y)$ combines this squared error of the expert subsequence $\hat{y}_{\geq j}^e$ and the query cost α_j .

6.2 Baselines

To compare the cost-accuracy tradeoffs achieved by partial deferral compared with whole-sequence deferral, we consider three confidence-thresholding baselines—`ChowSum`, `ChowMean`, and `ChowQuantile`—which defer the entire sequence based on the sum, mean, or a chosen quantile of token-level confidence scores computed over the predicted sequence. For TSP and XSUM ($|\mathcal{V}| < \infty$), the per-token score is the negative log-softmax; for MWP ($\mathcal{V} = \mathbb{R}$), it is the Monte Carlo dropout variance. `WholeModelEmbed` is a model-based whole-sequence rejector trained to predict whether the expert is more accurate than the predictor (Gupta et al., 2024).

For partial deferral, we compare our model-based rejectors against confidence-based methods at both granularities. At the token level, `TokenwiseScore` defers by thresholding token-level confidence scores, and `TokenwiseEntropy` defers by thresholding the entropy of the predictive distribution. In the one-time setting, `OneTimeScore` and `OneTimeEntropy` select a single handoff position based on the highest token-level confidence and predictive entropy, respectively. Entropy-based baselines apply only to XSUM and TSP, where the output vocabulary \mathcal{V} is finite. Formal expressions of these baselines are provided in Appendix C.

Table 1: Area under the deferral curve (AUDC; lower is better) and percentage improvement relative to a random rejector on TSP, XSUM, and MWP. *Random* flips a biased coin to defer; *Optimal* is an oracle that minimizes loss at each deferral budget. Bold indicates the best result (ties bolded) within each block (Whole, One-time, Token-level). Values are mean (std) over five runs (100 test instances per run). **OneTimeModel** uses the best-performing \mathcal{L}^ψ variant (see Figure 2).

Method	TSP		XSUM		MWP	
	AUDC	% Improvement	AUDC	% Improvement	AUDC	% Improvement
Random	306.12(6.31)	0.00 (0.00)	1433.55 (36.98)	0.00 (0.00)	555.33 (174.75)	0.00 (0.00)
Optimal	0.00(0.00)	100.00 (0.00)	1212.00 (46.85)	15.48 (1.50)	36.66 (4.34)	93.01 (1.47)
Whole Deferrals						
ChowMean	287.01(7.73)	6.23(2.14)	1430.52 (19.09)	0.13 (3.48)	521.75 (151.71)	5.26 (9.92)
ChowSum	287.01(7.73)	6.23(2.14)	1431.41 (19.65)	0.06 (3.50)	521.75 (151.71)	5.26 (9.92)
ChowQuantile 0	301.18(9.40)	1.63(1.18)	1432.28 (25.89)	-0.01 (3.89)	528.02 (151.50)	3.91 (9.25)
ChowQuantile 0.4	287.74(5.91)	6.00(1.16)	1436.10 (24.23)	-0.27 (3.80)	528.02 (151.50)	3.91 (9.25)
ChowQuantile 0.8	288.86(9.35)	5.65(2.12)	1434.48 (19.32)	-0.15 (3.40)	528.02 (151.50)	3.91 (9.25)
ChowQuantile 1.0	295.71(6.12)	3.39(1.42)	1427.27 (18.91)	0.35 (3.50)	528.02 (151.50)	3.91 (9.25)
WholeModelEmbed	307.88(8.73)	-0.58(2.02)	1434.23 (21.57)	-0.11 (3.81)	576.24 (160.28)	-5.28 (15.09)
One-time Deferrals						
OneTimeModel	270.92(10.67)	11.52(2.41)	1398.39(22.84)	2.35 (4.03)	508.82 (143.39)	7.23 (11.80)
OneTimeScore	319.79(14.53)	-4.44(3.63)	1433.41(26.82)	-1.50 (2.13)	521.64 (134.83)	4.46 (10.14)
OneTimeEntropy	324.23(13.48)	-5.93(4.15)	1442.92(24.92)	-1.75 (2.38)	-	-
Token-level Deferrals						
TokenwiseModel	-	-	1323.92 (25.34)	7.63 (0.93)	412.45 (131.43)	25.78 (1.33)
TokenwiseScore	-	-	1354.78 (31.87)	5.48 (0.97)	707.51 (203.38)	-28.50 (6.20)
TokenwiseEntropy	-	-	1360.41 (31.50)	5.09 (0.63)	-	-

6.3 Evaluation

We evaluate our methods using *deferral curves*, which plot the system loss against the number of deferred tokens using various thresholds of the rejector score $r(x)$ (see Figure 1). Loss is task-specific: for TSP, it is the percentage increase in tour length relative to the expert; for XSUM, it is $1 - \text{ROUGE1}$; and for MWP, it is the squared error $\|y - \hat{y}\|_2^2$. The area under the deferral curve (AUDC) summarizes the cost-quality tradeoff, and we also report the percentage improvement in AUDC over a random rejector, whose trade-off is linear. Thresholds do not directly determine rejection decisions in the one-time setting; to obtain similar curves, we adopt the following policy: if $g_{L+1}(x)$ (the score of the “no deferral” action) exceeds a threshold, the predictor completes the sequence, otherwise we defer at $\arg \max_{j \in \mathcal{J}} g_j(x)$. All results are averaged over five runs, each with 100 test instances.

6.4 Comparison with other deferral methods

Table 1 shows that model-based token-level and one-time deferral schemes outperform whole-sequence baselines (both model- and confidence-based); where applicable, token-level deferral attains the best AUDC. Within each type of granularity, model-based rejectors consistently exceed their confidence-thresholding counterparts. In XSUM, even confidence-based token-level deferral surpasses all whole-sequence methods, highlighting the advantage of fine-grained deferral. Gains for one-time deferral on TSP are modest, which we attribute to the non-autoregressive expert that cannot act on partial subsequences. By contrast, in XSUM and MWP, partial deferral yields markedly better cost-accuracy trade-offs.

6.5 Size of \mathcal{J} for One time Deferral

Additionally, we train one-time rejectors with \mathcal{L}^ψ with varying candidate sets of deferral points \mathcal{J} to assess how the number of allowable handoff positions affects cost-effectiveness, particularly on XSUM and TSP where the sequence length L is large. For both tasks, \mathcal{J} is a uniform grid over $\{1, \dots, L+1\}$ (with $L+1$ denoting “no deferral”), and we vary the grid granularity. Figure 2 demonstrates the need for a modified one-time deferral loss function. The model trained with all token positions ($|\mathcal{J}| = L + 1$) is not the most optimal

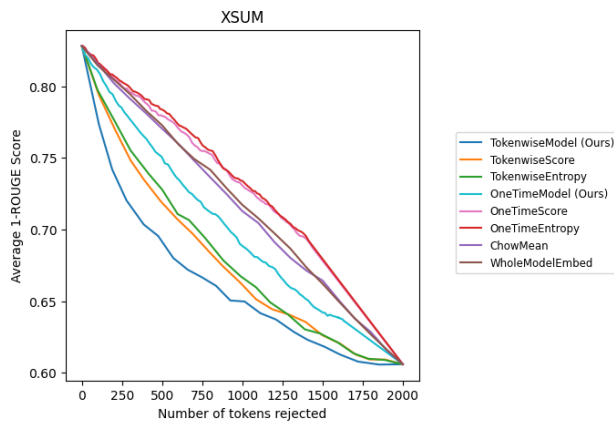


Figure 1: Deferral Curve for XSUM (closer to the lower left corner is better). See Appendix E for deferral curves of other tasks.

choice with the suboptimality exacerbated in the XSUM experiments. One-time rejectors are generally more cost-effective than its corresponding confidence-based rejectors regardless of the size of \mathcal{J} .

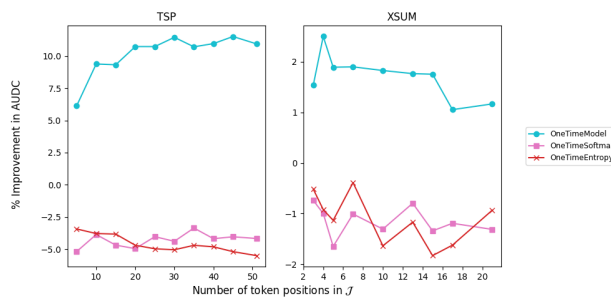


Figure 2: Plots of Size of \mathcal{J} against percentage improvement in AUDC relative to the random baseline for TSP (on the left) and XSUM (on the right). See Appendix G for exact AUDC values.

7 Discussion

We have introduced partial rejections as a way to improve the cost-effectiveness of a learning to defer system and proposed two model-based methods to support granular rejections. This work raises numerous interesting questions. We have currently proposed partial deferral with access to one expert, however, it would be interesting to extend this to the case with multiple experts. It would also be valuable to explore other types of partial deferrals with granularities between token-level and one-time deferrals. A rejector, for example, could select contiguous parts of a sequence to reject. Finally, studying partial rejections for larger outputs like protein structures would also be insightful.

References

- Naoki Abe, Bianca Zadrozny, and John Langford. An iterative method for multi-class cost-sensitive learning. In *Proceedings of the tenth ACM SIGKDD international conference on Knowledge discovery and data mining*, pp. 3–11, 2004.
- Zeynep Akata, Dan Balliet, Maarten De Rijke, Frank Dignum, Virginia Dignum, Gusztai Eiben, Antske Fokkens, Davide Grossi, Koen Hindriks, Holger Hoos, et al. A research agenda for hybrid intelligence:

- augmenting human intellect with collaborative, adaptive, responsible, and explainable artificial intelligence. *Computer*, 53(8):18–28, 2020.
- Kiana Alikhademi, Emma Drobina, Diandra Prioleau, Brianna Richardson, Duncan Purves, and Juan E Gilbert. A review of predictive policing from the perspective of fairness. *Artificial Intelligence and Law*, pp. 1–17, 2022.
- Omur Asan, Alparslan Emrah Bayrak, Avishek Choudhury, et al. Artificial intelligence and human trust in healthcare: focus on clinicians. *Journal of medical Internet research*, 22(6):e15154, 2020.
- Peter L Bartlett and Marten H Wegkamp. Classification with a reject option using a hinge loss. *Journal of Machine Learning Research*, 9(8), 2008.
- Peter L Bartlett, Michael I Jordan, and Jon D McAuliffe. Convexity, classification, and risk bounds. *Journal of the American Statistical Association*, 101(473):138–156, 2006.
- Samy Bengio, Oriol Vinyals, Navdeep Jaitly, and Noam Shazeer. Scheduled sampling for sequence prediction with recurrent neural networks. *Advances in neural information processing systems*, 28, 2015.
- Federico Berto, Chuanbo Hua, Junyoung Park, Laurin Luttmann, Yining Ma, Fanchen Bu, Jiarui Wang, Haoran Ye, Minsu Kim, Sanghyeok Choi, et al. RL4co: an extensive reinforcement learning for combinatorial optimization benchmark. *arXiv preprint arXiv:2306.17100*, 2023.
- Tom Brown, Benjamin Mann, Nick Ryder, Melanie Subbiah, Jared D Kaplan, Prafulla Dhariwal, Arvind Neelakantan, Pranav Shyam, Girish Sastry, Amanda Askell, et al. Language models are few-shot learners. *Advances in neural information processing systems*, 33:1877–1901, 2020.
- Yuzhou Cao, Tianchi Cai, Lei Feng, Lihong Gu, Jinjie Gu, Bo An, Gang Niu, and Masashi Sugiyama. Generalizing consistent multi-class classification with rejection to be compatible with arbitrary losses. *Advances in neural information processing systems*, 35:521–534, 2022.
- Lingjiao Chen, Matei Zaharia, and James Zou. Frugalgpt: How to use large language models while reducing cost and improving performance. *arXiv preprint arXiv:2305.05176*, 2023.
- Xin Cheng, Yuzhou Cao, Haobo Wang, Hongxin Wei, Bo An, and Lei Feng. Regression with cost-based rejection. *Advances in Neural Information Processing Systems*, 36, 2024.
- Chi-Keung Chow. An optimum character recognition system using decision functions. *IRE Transactions on Electronic Computers*, (4):247–254, 1957.
- Yu-An Chung, Hsuan-Tien Lin, and Shao-Wen Yang. Cost-aware pre-training for multiclass cost-sensitive deep learning. *arXiv preprint arXiv:1511.09337*, 2015.
- Corinna Cortes, Giulia DeSalvo, and Mehryar Mohri. Learning with rejection. In *Algorithmic Learning Theory: 27th International Conference, ALT 2016, Bari, Italy, October 19-21, 2016, Proceedings 27*, pp. 67–82. Springer, 2016.
- Pierre Courtiol, Charles Maussion, Matahi Moarii, Elodie Pronier, Samuel Pilcer, Meriem Sefta, Pierre Manceron, Sylvain Toldo, Mikhail Zaslavskiy, Nolwenn Le Stang, et al. Deep learning-based classification of mesothelioma improves prediction of patient outcome. *Nature medicine*, 25(10):1519–1525, 2019.
- Justas Dauparas, Ivan Anishchenko, Nathaniel Bennett, Hua Bai, Robert J Ragothe, Lukas F Milles, Basile IM Wicky, Alexis Courbet, Rob J de Haas, Neville Bethel, et al. Robust deep learning-based protein sequence design using proteinmpnn. *Science*, 378(6615):49–56, 2022.
- Dominik Dellermann, Philipp Ebel, Matthias Söllner, and Jan Marco Leimeister. Hybrid intelligence. *Business & Information Systems Engineering*, 61(5):637–643, 2019.
- Dujian Ding, Ankur Mallick, Chi Wang, Robert Sim, Subhabrata Mukherjee, Victor Ruhle, Laks VS Lakshmanan, and Ahmed Hassan Awadallah. Hybrid llm: Cost-efficient and quality-aware query routing. *arXiv preprint arXiv:2404.14618*, 2024.

- Julia Dressel and Hany Farid. The accuracy, fairness, and limits of predicting recidivism. *Science advances*, 4(1):eaa05580, 2018.
- Ran El-Yaniv and Yair Wiener. On the foundations of noise-free selective classification. *Journal of Machine Learning Research*, 11(5), 2010.
- Yarin Gal and Zoubin Ghahramani. Dropout as a bayesian approximation: Representing model uncertainty in deep learning. In *international conference on machine learning*, pp. 1050–1059. PMLR, 2016.
- Yonatan Geifman and Ran El-Yaniv. Selective classification for deep neural networks. *Advances in neural information processing systems*, 30, 2017.
- Yonatan Geifman and Ran El-Yaniv. Selectivenet: A deep neural network with an integrated reject option. In *International conference on machine learning*, pp. 2151–2159. PMLR, 2019.
- Aritra Ghosh, Himanshu Kumar, and P Shanti Sastry. Robust loss functions under label noise for deep neural networks. In *Proceedings of the AAAI conference on artificial intelligence*, volume 31, 2017.
- Neha Gupta, Harikrishna Narasimhan, Wittawat Jitkrittum, Ankit Singh Rawat, Aditya Krishna Menon, and Sanjiv Kumar. Language model cascades: Token-level uncertainty and beyond. *arXiv preprint arXiv:2404.10136*, 2024.
- Patrick Hemmer, Lukas Thede, Michael Vössing, Johannes Jakubik, and Niklas Kühl. Learning to defer with limited expert predictions. In *Proceedings of the AAAI Conference on Artificial Intelligence*, volume 37, pp. 6002–6011, 2023.
- Dongfu Jiang, Xiang Ren, and Bill Yuchen Lin. Llm-blender: Ensembling large language models with pairwise ranking and generative fusion. In *Proceedings of the 61st Annual Meeting of the Association for Computational Linguistics (Volume 1: Long Papers)*, pp. 14165–14178, 2023.
- Wenming Jiang, Ying Zhao, and Zehan Wang. Risk-controlled selective prediction for regression deep neural network models. In *2020 International Joint Conference on Neural Networks (IJCNN)*, pp. 1–8. IEEE, 2020.
- John Jumper, Richard Evans, Alexander Pritzel, Tim Green, Michael Figurnov, Olaf Ronneberger, Kathryn Tunyasuvunakool, Russ Bates, Augustin Zidek, Anna Potapenko, et al. Highly accurate protein structure prediction with alphafold. *nature*, 596(7873):583–589, 2021.
- Ece Kamar. Directions in hybrid intelligence: Complementing ai systems with human intelligence. In *IJCAI*, pp. 4070–4073, 2016.
- Jacob Devlin Ming-Wei Chang Kenton and Lee Kristina Toutanova. Bert: Pre-training of deep bidirectional transformers for language understanding. In *Proceedings of naacL-HLT*, volume 1, pp. 2. Minneapolis, Minnesota, 2019.
- Justin Ker, Lipo Wang, Jai Rao, and Tchoyoson Lim. Deep learning applications in medical image analysis. *Ieee Access*, 6:9375–9389, 2017.
- Alex M Lamb, Anirudh Goyal ALIAS PARTH GOYAL, Ying Zhang, Saizheng Zhang, Aaron C Courville, and Yoshua Bengio. Professor forcing: A new algorithm for training recurrent networks. *Advances in neural information processing systems*, 29, 2016.
- Hsuan-Tien Lin. Reduction from cost-sensitive multiclass classification to one-versus-one binary classification. In *Asian Conference on Machine Learning*, pp. 371–386. PMLR, 2015.
- Keming Lu, Hongyi Yuan, Runji Lin, Junyang Lin, Zheng Yuan, Chang Zhou, and Jingren Zhou. Routing to the expert: Efficient reward-guided ensemble of large language models. *arXiv preprint arXiv:2311.08692*, 2023.

- Mansoureh Maadi, Hadi Akbarzadeh Khorshidi, and Uwe Aickelin. A review on human–ai interaction in machine learning and insights for medical applications. *International journal of environmental research and public health*, 18(4):2121, 2021.
- David Madras, Toni Pitassi, and Richard Zemel. Predict responsibly: improving fairness and accuracy by learning to defer. *Advances in neural information processing systems*, 31, 2018.
- Anqi Mao, Mehryar Mohri, and Yutao Zhong. Cross-entropy loss functions: Theoretical analysis and applications. In *International conference on Machine learning*, pp. 23803–23828. PMLR, 2023.
- Anqi Mao, Mehryar Mohri, and Yutao Zhong. Predictor-rejector multi-class abstention: Theoretical analysis and algorithms. In *International Conference on Algorithmic Learning Theory*, pp. 822–867. PMLR, 2024a.
- Anqi Mao, Mehryar Mohri, and Yutao Zhong. Regression with multi-expert deferral. *arXiv preprint arXiv:2403.19494*, 2024b.
- Anqi Mao, Mehryar Mohri, and Yutao Zhong. Theoretically grounded loss functions and algorithms for score-based multi-class abstention. In *International Conference on Artificial Intelligence and Statistics*, pp. 4753–4761. PMLR, 2024c.
- Andreas Maurer. A vector-contraction inequality for rademacher complexities. In *Algorithmic Learning Theory: 27th International Conference, ALT 2016, Bari, Italy, October 19-21, 2016, Proceedings 27*, pp. 3–17. Springer, 2016.
- Hussein Mozannar and David Sontag. Consistent estimators for learning to defer to an expert. In *International Conference on Machine Learning*, pp. 7076–7087. PMLR, 2020.
- Jinseok Nam, Eneldo Loza Mencia, Hyunwoo J Kim, and Johannes Fürnkranz. Maximizing subset accuracy with recurrent neural networks in multi-label classification. *Advances in neural information processing systems*, 30, 2017.
- Harikrishna Narasimhan, Wittawat Jitkrittum, Ankit Singh Rawat, Seungyeon Kim, Neha Gupta, Aditya Krishna Menon, and Sanjiv Kumar. Faster cascades via speculative decoding. *arXiv preprint arXiv:2405.19261*, 2024.
- Shashi Narayan, Shay B Cohen, and Mirella Lapata. Don’t give me the details, just the summary! topic-aware convolutional neural networks for extreme summarization. *arXiv preprint arXiv:1808.08745*, 2018.
- Erik Nijkamp, Jeffrey A Ruffolo, Eli N Weinstein, Nikhil Naik, and Ali Madani. Progen2: exploring the boundaries of protein language models. *Cell systems*, 14(11):968–978, 2023.
- Colin Raffel, Noam Shazeer, Adam Roberts, Katherine Lee, Sharan Narang, Michael Matena, Yanqi Zhou, Wei Li, and Peter J Liu. Exploring the limits of transfer learning with a unified text-to-text transformer. *Journal of machine learning research*, 21(140):1–67, 2020.
- Harish G. Ramaswamy, Ambuj Tewari, and Shivani Agarwal. Consistent algorithms for multiclass classification with an abstain option. *Electronic Journal of Statistics*, 12(1), Jan 2018. doi: 10.1214/17-ejs1388.
- Jesse Read, Bernhard Pfahringer, Geoffrey Holmes, and Eibe Frank. Classifier chains: A review and perspectives. *Journal of Artificial Intelligence Research*, 70:683–718, 2021.
- Christopher Rigano. Using artificial intelligence to address criminal justice needs. *National Institute of Justice Journal*, 280(1-10):17, 2019.
- Florian Schmidt. Generalization in generation: A closer look at exposure bias. *arXiv preprint arXiv:1910.00292*, 2019.
- Abhin Shah, Yuheng Bu, Joshua K Lee, Subhro Das, Rameswar Panda, Prasanna Sattigeri, and Gregory W Wornell. Selective regression under fairness criteria. In *International Conference on Machine Learning*, pp. 19598–19615. PMLR, 2022.

- Tal Shnitzer, Anthony Ou, Mírian Silva, Kate Soule, Yuekai Sun, Justin Solomon, Neil Thompson, and Mikhail Yurochkin. Large language model routing with benchmark datasets. *arXiv preprint arXiv:2309.15789*, 2023.
- Han-Hsing Tu and Hsuan-Tien Lin. One-sided support vector regression for multiclass cost-sensitive classification. In *ICML*, volume 2, pp. 5, 2010.
- Rajeev Verma and Eric Nalisnick. Calibrated learning to defer with one-vs-all classifiers. In *International Conference on Machine Learning*, pp. 22184–22202. PMLR, 2022.
- Rajeev Verma, Daniel Barrejón, and Eric Nalisnick. Learning to defer to multiple experts: Consistent surrogate losses, confidence calibration, and conformal ensembles. In *International Conference on Artificial Intelligence and Statistics*, pp. 11415–11434. PMLR, 2023.
- Oriol Vinyals, Meire Fortunato, and Navdeep Jaitly. Pointer networks. *Advances in neural information processing systems*, 28, 2015.
- Paul Viola and Michael Jones. Rapid object detection using a boosted cascade of simple features. In *Proceedings of the 2001 IEEE computer society conference on computer vision and pattern recognition. CVPR 2001*, volume 1, pp. I–I. Ieee, 2001.
- Congchao Wang, Sean Augenstein, Keith Rush, Wittawat Jitkrittum, Harikrishna Narasimhan, Ankit Singh Rawat, Aditya Krishna Menon, and Alec Go. Cascade-aware training of language models. *arXiv preprint arXiv:2406.00060*, 2024.
- Jingxue Wang, Huali Cao, John ZH Zhang, and Yifei Qi. Computational protein design with deep learning neural networks. *Scientific reports*, 8(1):1–9, 2018.
- Ronald J. Williams and David Zipser. A learning algorithm for continually running fully recurrent neural networks. *Neural Computation*, 1(2):270–280, 1989.
- Ming Yuan and Marten Wegkamp. Classification methods with reject option based on convex risk minimization. *Journal of Machine Learning Research*, 11(1), 2010.
- Murong Yue, Jie Zhao, Min Zhang, Liang Du, and Ziyu Yao. Large language model cascades with mixture of thoughts representations for cost-efficient reasoning. *arXiv preprint arXiv:2310.03094*, 2023.
- Ahmed Zaoui, Christophe Denis, and Mohamed Hebiri. Regression with reject option and application to knn. *Advances in Neural Information Processing Systems*, 33:20073–20082, 2020.

A Proofs for Section 3

A.1 Proof of Proposition A.1

Proposition A.1. *If ϕ is binary classification calibrated and convex, $\mathcal{L}^\phi(h, r, x, y)$ is a convex upper bound of $\mathcal{L}^{\text{Token}}(h, r, x, y)$ upto some scale γ*

Proof. It is easy to see that $\mathcal{L}_j^\phi(h, r, x, y)$ is convex with respect to r as long as $\phi(\cdot)$ is convex. Since ϕ is binary classification calibrated, there is a constant γ such that $\gamma\phi(z) \geq \mathbf{1}_{z \leq 0}$ by Lemma 3 from Bartlett et al. (2006). Therefore, $\gamma\mathcal{L}^\phi(h, r, x, y) \geq \mathcal{L}^{\text{Token}}(h, r, x, y)$.

□

A.2 Proof of Lemma 3.1

Lemma A.2. Let $0 < \bar{c} \leq c_j(x, \hat{y}_{<j}, y) \leq \bar{C} < \infty$ for all j , $0 \leq l(y, \hat{y}_j^h) \leq \bar{l} < \infty$, and ϕ be a binary surrogate loss that satisfies the following inequality for any distribution over $\mathcal{X} \times \{-1, 1\}$ and any measurable function f :

$$\mathcal{R}_{\text{binary } 0-1}(f) - \mathcal{R}_{\text{binary } 0-1}^*(f) \leq \Gamma(\mathcal{R}_{\text{binary } \phi}(f) - \mathcal{R}_{\text{binary } \phi}^*(f))$$

where $\mathcal{R}_{\text{binary } 0-1}$ is the binary 0-1 risk and $\Gamma: \mathbb{R}^+ \rightarrow \mathbb{R}^+$ is a non-decreasing concave function. Then, for any measurable r and any h , the following inequality holds for any distribution over $\mathcal{X} \times \mathcal{Y}$:

$$\mathcal{R}_{\text{Token}}(r, h) - \mathcal{R}_{\text{Token}}^*(h) \leq \tilde{\Gamma}(\mathcal{R}_{\phi}(r, h) - \mathcal{R}_{\phi}^*(h))$$

where $\tilde{\Gamma}(z) = (\bar{l} + \bar{C}) \Gamma(\frac{z}{\bar{c}})$, $\mathcal{R}_{\text{Token}}^*(h) := \inf_r \mathcal{R}_{\text{Token}}(r, h)$, and $\mathcal{R}_{\phi}^*(h) := \inf_r \mathcal{R}_{\phi}(r, h)$

Proof. Let $C_{\text{Token}}(r, h, x) = \mathbb{E}_{y \sim \mathcal{P}_{\mathcal{Y}|X=x}}[\mathcal{L}^{\text{Token}}(h, r, x, y)]$ be the pointwise $\mathcal{L}^{\text{Token}}$ -risk for a given x and predictor h and let $C_{\text{Token}}^*(h, x) = \inf_r C_{\text{Token}}(r, h, x)$ be the optimal pointwise $\mathcal{L}^{\text{Token}}$ -risk for a given x and predictor h . Similarly, let $C_{\phi}(r, h, x) = \mathbb{E}_{y \sim \mathcal{P}_{\mathcal{Y}|X=x}}[\mathcal{L}^{\phi}(h, r, x, y)]$ be the pointwise \mathcal{L}^{ϕ} -risk for a given x and predictor h and $C_{\phi}^*(h, x) = \inf_r C_{\phi}(r, h, x)$ be the optimal pointwise \mathcal{L}^{ϕ} -risk. For any measurable function r , the excess pointwise \mathcal{L}^{ϕ} -risk can be characterized by:

$$\begin{aligned} & C_{\text{Token}}(r, h, x) - C_{\text{Token}}^*(h, x) \\ &= \frac{1}{L} \sum_{j=1}^L \mathbb{E}_{y \sim \mathcal{P}_{\mathcal{Y}|X=x}} [l(y, \hat{y}_j^h)] \mathbf{1}_{r(x, \hat{y}_{<j}) \leq 0} + \mathbb{E}_{y \sim \mathcal{P}_{\mathcal{Y}|X=x}} [c_j(x, \hat{y}_{<j}, y)] \mathbf{1}_{r(x, \hat{y}_{<j}) > 0} \\ & \quad - \frac{1}{L} \inf_{\tilde{r}} \left\{ \sum_{j=1}^L \mathbb{E}_{y \sim \mathcal{P}_{\mathcal{Y}|X=x}} [l(y, \hat{y}_j^h)] \mathbf{1}_{\tilde{r}(x, \hat{y}_{<j}) \leq 0} + \mathbb{E}_{y \sim \mathcal{P}_{\mathcal{Y}|X=x}} [c_j(x, \hat{y}_{<j}, y)] \mathbf{1}_{\tilde{r}(x, \hat{y}_{<j}) > 0} \right\} \end{aligned}$$

Let $A_j = \mathbb{E}_{y \sim \mathcal{P}_{\mathcal{Y}|X=x}} [l(y, \hat{y}_{<j})]$ and $B_j = \mathbb{E}_{y \sim \mathcal{P}_{\mathcal{Y}|X=x}} [c_j(x, \hat{y}_{<j}, y)]$

$$\begin{aligned} & C_{\text{Token}}(r, h, x) - C_{\text{Token}}^*(h, x) \\ &= \frac{1}{L} \sum_{j=1}^L A_j \mathbf{1}_{r_j(x, \hat{y}_{<j}) \leq 0} + B_j \mathbf{1}_{r_j(x, \hat{y}_{<j}) > 0} - \frac{1}{L} \inf_{\tilde{r}} \left\{ \sum_{j=1}^L A_j \mathbf{1}_{\tilde{r}_j(x, \hat{y}_{<j}) \leq 0} + B_j \mathbf{1}_{\tilde{r}_j(x, \hat{y}_{<j}) > 0} \right\} \\ &= \frac{1}{L} \sum_{j=1}^L (A_j + B_j) \left(\frac{A_j}{A_j + B_j} \mathbf{1}_{r_j(x, \hat{y}_{<j}) \leq 0} + \frac{B_j}{A_j + B_j} \mathbf{1}_{r_j(x, \hat{y}_{<j}) > 0} \right) \\ & \quad - \frac{1}{L} \inf_{\tilde{r}} \left\{ \sum_{j=1}^L (A_j + B_j) \left(\frac{A_j}{A_j + B_j} \mathbf{1}_{\tilde{r}_j(x, \hat{y}_{<j}) \leq 0} + \frac{B_j}{A_j + B_j} \mathbf{1}_{\tilde{r}_j(x, \hat{y}_{<j}) > 0} \right) \right\} \\ &\leq \frac{(\bar{l} + \bar{C})}{L} \sum_{j=1}^L \frac{A_j}{A_j + B_j} \mathbf{1}_{r_j(x, \hat{y}_{<j}) \leq 0} + \frac{B_j}{A_j + B_j} \mathbf{1}_{r_j(x, \hat{y}_{<j}) > 0} \\ & \quad - \frac{(\bar{l} + \bar{C})}{L} \inf_{\tilde{r}} \left\{ \sum_{j=1}^L \frac{A_j}{A_j + B_j} \mathbf{1}_{\tilde{r}_j(x, \hat{y}_{<j}) \leq 0} + \frac{B_j}{A_j + B_j} \mathbf{1}_{\tilde{r}_j(x, \hat{y}_{<j}) > 0} \right\} \end{aligned}$$

Consider a feature space $\tilde{\mathcal{X}} = \mathcal{X} \times \mathcal{Y}^*$ and output space $\tilde{\mathcal{Y}} = \{-1, 1\}$. Let the distribution on $\tilde{\mathcal{X}}$ be uniform over $\{\tilde{x}_1, \dots, \tilde{x}_L\}$ where $\tilde{x}_j = (x, \hat{y}_{<j})$ with $\frac{1}{L}$ mass on each point on the set. Let $P(\tilde{Y} = -1 | \tilde{X} = \tilde{x}_j) = \frac{A_j}{A_j + B_j}$ and f be a measurable function such that $f(\tilde{x}_j) = r_j(\tilde{x}_j) = r_j(x, \hat{y}_{<j})$

Under this distribution,

$$\begin{aligned}\mathcal{R}^{\text{binary } 0-1}(r) &= \frac{1}{L} \sum_{j=1}^L \frac{A_j}{A_j + B_j} \mathbf{1}_{r_j(x, \hat{y}_{<j}) \leq 0} + \frac{B_j}{A_j + B_j} \mathbf{1}_{r_j(x, \hat{y}_{<j}) > 0} \\ \mathcal{R}^*_{\text{binary } 0-1} &= \frac{1}{L} \inf_{\tilde{r}} \left\{ \sum_{j=1}^L \frac{A_j}{A_j + B_j} \mathbf{1}_{\tilde{r}_j(x, \hat{y}_{<j}) \leq 0} + \frac{B_j}{A_j + B_j} \mathbf{1}_{\tilde{r}_j(x, \hat{y}_{<j}) > 0} \right\} \\ \mathcal{R}^{\text{binary } \phi}(r) &= \frac{1}{L} \sum_{j=1}^L \frac{A_j}{A_j + B_j} \phi(r_j(x, \hat{y}_{<j})) + \frac{B_j}{A_j + B_j} \phi(-r_j(x, \hat{y}_{<j})) \\ \mathcal{R}^*_{\text{binary } \phi} &= \frac{1}{L} \inf_{\tilde{r}} \left\{ \sum_{j=1}^L \frac{A_j}{A_j + B_j} \phi(\tilde{r}_j(x, \hat{y}_{<j})) + \frac{B_j}{A_j + B_j} \phi(-\tilde{r}_j(x, \hat{y}_{<j})) \right\}\end{aligned}$$

From the theorem statement,

$$\begin{aligned}C_{\text{Token}}(r, h, x) - C^*_{\text{Token}}(h, x) &\leq \frac{(\bar{l} + \bar{C})}{L} \sum_{j=1}^L \frac{A_j}{A_j + B_j} \mathbf{1}_{r_j(x, \hat{y}_{<j}) \leq 0} + \frac{B_j}{A_j + B_j} \mathbf{1}_{r_j(x, \hat{y}_{<j}) > 0} \\ &\quad - \frac{(\bar{l} + \bar{C})}{L} \inf_{\tilde{r}} \left\{ \sum_{j=1}^L \frac{A_j}{A_j + B_j} \mathbf{1}_{\tilde{r}_j(x, \hat{y}_{<j}) \leq 0} + \frac{B_j}{A_j + B_j} \mathbf{1}_{\tilde{r}_j(x, \hat{y}_{<j}) > 0} \right\} \\ &\leq (\bar{l} + \bar{C}) \Gamma \left(\frac{\sum_{j=1}^L \frac{A_j \phi(r_j(x, \hat{y}_{<j})) + B_j \phi(-r_j(x, \hat{y}_{<j}))}{L(A_j + B_j)}}{\inf_{\tilde{r}} \left\{ \sum_{j=1}^L \frac{A_j \phi(\tilde{r}_j(x, \hat{y}_{<j})) + B_j \phi(-\tilde{r}_j(x, \hat{y}_{<j}))}{L(A_j + B_j)} \right\}} \right) \\ &\leq (\bar{l} + \bar{C}) \Gamma \left(\frac{\sum_{j=1}^L \frac{A_j \phi(r_j(x, \hat{y}_{<j})) + B_j \phi(-r_j(x, \hat{y}_{<j}))}{L\bar{c}}}{\inf_{\tilde{r}} \left\{ \sum_{j=1}^L \frac{A_j \phi(\tilde{r}_j(x, \hat{y}_{<j})) + B_j \phi(-\tilde{r}_j(x, \hat{y}_{<j}))}{L\bar{c}} \right\}} \right) \\ &= (\bar{l} + \bar{C}) \Gamma \left(\frac{C_\phi(r, h, x) - C^*_\phi(h, x)}{\bar{c}} \right)\end{aligned}$$

Let $\tilde{\Gamma}(z) = (\bar{l} + \bar{C}) \Gamma\left(\frac{z}{\bar{c}}\right)$. Then,

$$\begin{aligned}\mathcal{R}_{\text{Token}}(r, h) - \mathcal{R}^*_{\text{Token}}(h) &= \mathbb{E}_{x \sim \mathcal{P}_X} [C_{\text{Token}}(r, h, x) - C^*_{\text{Token}}(h, x)] \\ &\leq \mathbb{E}_{x \sim \mathcal{P}_X} [\tilde{\Gamma}(C_\phi(r, h, x) - C^*_\phi(h, x))] \\ &\stackrel{(a)}{\leq} \tilde{\Gamma} \left(\mathbb{E}_{x \sim \mathcal{P}_X} [C_\phi(r, h, x) - C^*_\phi(h, x)] \right) \\ &\stackrel{(b)}{=} \tilde{\Gamma}(\mathcal{R}_\phi(r, h) - \mathcal{R}^*_\phi(h))\end{aligned}$$

(a) by Jensen's inequality since $\tilde{\Gamma}$ is concave, (b) since the infimum is taken over all measurable functions $\mathcal{R}^*_\phi(h) = \mathbb{E}_{x \sim \mathcal{P}_X} [C^*_\phi(h, x)]$

□

A.3 Proof of Theorem 3.2

Definition A.3 (Classification Calibration). Let $\eta(x) = \mathbb{P}[Y = 1 | X = x]$ and $\mathcal{R}_\phi(f) = \mathbb{E}_{x \sim \mathcal{P}_X} [C_\phi(\eta(x), f(x))]$ where $C_\phi(\eta, t) = \eta\phi(t) + (1 - \eta)\phi(-t)$. ϕ is considered binary classification calibrated if $C_\phi^-(\eta) - C_\phi^*(\eta) > 0$ for all $\eta \neq \frac{1}{2}$ where $C_\phi^-(\eta) = \inf_{t: t(\eta - \frac{1}{2}) \leq 0} C_\phi(\eta, t)$ and $C_\phi^*(\eta) = \inf_{t \in \mathbb{R}} C_\phi(\eta, t)$

Theorem A.4 (Consistency). *If $0 < \bar{c} \leq c_j(x, \hat{y}_{<j}, y) \leq \bar{C} < \infty$ for all j , $0 \leq l(y, \hat{y}_j^h) \leq \bar{l} < \infty$, and ϕ be binary classification calibrated, then, for a fixed h , \mathcal{L}^ϕ is a Bayes consistent surrogate for $\mathcal{L}^{\text{Token}}$*

Proof. Since ϕ is binary classification calibrated, we know that $\mathcal{R}_{\text{binary } 0-1}(f) - \mathcal{R}_{\text{binary } 0-1}^* \leq \psi^{-1} \left(\mathcal{R}_{\text{binary } \phi}(f) - \mathcal{R}_{\text{binary } \phi}^* \right)$ where ψ is a non-decreasing convex function, making ψ^{-1} a non-decreasing concave function Bartlett et al. (2006). By Lemma 3.1, $\mathcal{R}_{\text{Token}}(r, h) - \mathcal{R}_{\text{Token}}^*(h) \leq \tilde{\Gamma} \left(\mathcal{R}_\phi(r, h) - \mathcal{R}_\phi^*(h) \right)$ where $\tilde{\Gamma}(z) = (1 + \bar{C}) \psi^{-1} \left(\frac{z}{\bar{c}} \right)$. If $\lim_{n \rightarrow \infty} \mathcal{R}_\phi(r_n, h) - \mathcal{R}_\phi^*(h) = 0$, then

$$\begin{aligned} \lim_{n \rightarrow \infty} \mathcal{R}_{\text{Token}}(r_n, h) - \mathcal{R}_{\text{Token}}^*(h) &\leq \lim_{n \rightarrow \infty} \tilde{\psi} \left(\mathcal{R}_\phi(r_n, h) - \mathcal{R}_\phi^*(h) \right) \\ &\stackrel{(a)}{=} (1 + \bar{C}) \psi \left(\lim_{n \rightarrow \infty} \frac{\mathcal{R}_\phi(r_n, h) - \mathcal{R}_\phi^*(h)}{\bar{c}} \right) \\ &= (1 + \bar{C}) \psi(0) \\ &\stackrel{(b)}{=} 0 \end{aligned}$$

(a) by continuity of ψ at 0 and (b) since $\psi(0) = 0$ Bartlett et al. (2006) □

A.4 Proof of Theorem 3.3

Theorem A.5. *Suppose $r \in \mathcal{F}$ which is composed of $\{\mathcal{F}_j\}_{j=1}^L$ such that $r_j \in \mathcal{F}_j$, $c_j(x) \leq \bar{C}$, and $l(y, \hat{y}_j^h) \leq \bar{l} < \infty$. If ϕ is ρ -lipschitz continuous, then with probability $1 - \delta$, the following upper bound holds for the empirical risk minimizer \hat{r}_n with respect to \mathcal{L}_ϕ for a fixed h :*

$$\mathcal{R}_\phi(\hat{r}_n, h) - \mathcal{R}_\phi^*(\mathcal{F}, h) \leq \frac{4\rho\sqrt{2(\bar{C}^2 + \bar{l}^2)}}{L} \sum_{j=1}^L \mathfrak{R}_n(\mathcal{F}_j) + (\bar{C} + \bar{l})\sqrt{\frac{2\log(\frac{2}{\delta})}{n}}$$

where $\mathcal{R}_\phi^*(\mathcal{F}, h) = \inf_{r \in \mathcal{F}} \mathcal{R}_\phi(r, h)$ and $\mathfrak{R}_n(\mathcal{F}_j)$ is the Rademacher Complexity of \mathcal{F}_j

Proof. Let $G_n = \sup_{r \in \mathcal{F}} \left[\mathcal{R}_\phi(r, h) - \widehat{\mathcal{R}}_\phi(r, h) \right]$, $G'_n = \sup_{r \in \mathcal{F}} \left[\widehat{\mathcal{R}}_\phi(r, h) - \mathcal{R}_\phi(r, h) \right]$, and $\mathcal{B} = \{(x, y) \mapsto \mathcal{L}^\phi(h, r, x, y) : r \in \mathcal{F}\}$.

If $z^i = (x^i, y^i)$, $G_n = g(z^1, \dots, z^n)$. Since $\left| g(z^1, \dots, z^i, \dots, z^n) - g(z^1, \dots, z^{i'}, \dots, z^n) \right| \leq \frac{\bar{C} + \bar{l}}{n}$, by applying McDiarmid's inequality

$$\begin{aligned} P \left(G_n > \frac{\epsilon}{2} \right) &\leq \exp \left\{ \frac{-2 \left(\frac{\epsilon}{2} - \mathbb{E}[G_n] \right)^2}{\sum_{i=1}^n \frac{(\bar{C} + \bar{l})^2}{n^2}} \right\} \\ &\leq \exp \left\{ \frac{-2n \left(\frac{\epsilon}{2} - 2\mathfrak{R}_n(\mathcal{B}) \right)^2}{(\bar{C} + \bar{l})^2} \right\} \\ &\stackrel{\text{def}}{=} \frac{\delta}{2} \end{aligned}$$

Similarly,

$$P \left(G'_n > \frac{\epsilon}{2} \right) \leq \exp \left\{ \frac{-2n \left(\frac{\epsilon}{2} - 2\mathfrak{R}_n(\mathcal{B}) \right)^2}{(\bar{C} + \bar{l})^2} \right\} = \frac{\delta}{2}$$

Let $\epsilon = 4\mathfrak{R}_n(\mathcal{B}) + (\bar{C} + \bar{l})\sqrt{\frac{2\log(\frac{2}{\delta})}{n}}$

$$\begin{aligned}
P(\mathcal{R}_\phi(\hat{r}_n, h) - \mathcal{R}_\phi^*(\mathcal{F}, h) > \epsilon) &\leq P\left(\sup_{r \in \mathcal{F}} |\mathcal{R}_\phi(r, h) - \hat{\mathcal{R}}_\phi(r, h)| > \frac{\epsilon}{2}\right) \\
&\leq P\left(G_n > \frac{\epsilon}{2}\right) + P\left(G'_n > \frac{\epsilon}{2}\right) \\
&\leq \delta
\end{aligned}$$

With at least probability $1 - \delta$, $\mathcal{R}_\phi(\hat{r}_n, h) - \mathcal{R}_\phi^*(\mathcal{F}, h) \leq 4\mathfrak{R}_n(\mathcal{B}) + (\bar{C} + \bar{l})\sqrt{\frac{2\log(\frac{2}{\delta})}{n}}$.

We can further bound $\mathfrak{R}_n(\mathcal{B})$ by $\mathfrak{R}_n(\mathcal{F}_j)$ if we show that \mathcal{L}^ϕ is Lipschitz continuous with respect to r

$$\begin{aligned}
&\|\mathcal{L}^\phi(h, r_1, x, y) - \mathcal{L}^\phi(h, r_2, x, y)\|_2^2 \\
&\leq \left\| \frac{1}{L} \sum_{j=1}^L l(y, \hat{y}_j^h) \phi(r_{1,j}(x, \hat{y}_{<j})) - l(y, \hat{y}_j^h) \phi(r_{2,j}(x, \hat{y}_{<j})) \right\|_2^2 \\
&+ \left\| \frac{1}{L} \sum_{j=1}^L c_j(x, \hat{y}_{<j}) \phi(-r_{1,j}(x, \hat{y}_{<j})) - c_j(x, \hat{y}_{<j}) \phi(-r_{2,j}(x, \hat{y}_{<j})) \right\|_2^2 \\
&\leq \frac{\bar{l}^2}{L^2} \sum_{j=1}^L \|\phi(r_{1,j}(x, \hat{y}_{<j})) - \phi(r_{2,j}(x, \hat{y}_{<j}))\|_2^2 + \frac{\bar{C}^2}{L^2} \sum_{j=1}^L \|\phi(-r_{1,j}(x, \hat{y}_{<j})) - \phi(-r_{2,j}(x, \hat{y}_{<j}))\|_2^2 \\
&\leq \frac{\rho^2(\bar{C}^2 + \bar{l}^2)}{L^2} \sum_{j=1}^L \|r_{1,j}(x, \hat{y}_{<j}) - r_{2,j}(x, \hat{y}_{<j})\|_2^2
\end{aligned}$$

By the extension of the Talagrand's Contraction Lemma Maurer (2016),

$$\mathfrak{R}_n(\mathcal{B}) \leq \frac{\rho\sqrt{2(\bar{C}^2 + \bar{l}^2)}}{L} \sum_{j=1}^L \mathfrak{R}_n(\mathcal{F}_j)$$

□

A.5 Proof of Corollary 3.4

Corollary A.6. *Suppose $r \in \mathcal{F}$ which is composed of $\{\mathcal{F}_j\}_{j=1}^L$ such that $r_j \in \mathcal{F}_j$, $0 < \bar{c} \leq c_j(x) \leq \bar{C}$, and $l(y, \hat{y}_j^h) \leq \bar{l} < \infty$. If ϕ is a ρ -lipschitz continuous binary classification-calibrated function, then with probability $1 - \delta$, the following upper bound on the excess risk with respect to $\mathcal{L}^{\text{Token}}$ holds for the empirical risk minimizer \hat{r}_n with respect to \mathcal{L}_ϕ for a fixed h :*

$$\mathcal{R}_{\text{Token}}(\hat{r}_n, h) - \mathcal{R}_{\text{Token}}^*(h) \leq \tilde{\Gamma}(\mathcal{B}(\mathcal{F}) + \mathcal{A}_\phi(\mathcal{F}, h))$$

where $\tilde{\Gamma} : \mathbb{R}^+ \rightarrow \mathbb{R}^+$, $\mathcal{B}(\mathcal{F}) = \frac{4\rho\sqrt{2(\bar{C}^2 + \bar{l}^2)}}{L} \sum_{j=1}^L \mathfrak{R}_n(\mathcal{F}_j) + (\bar{C} + \bar{l})\sqrt{\frac{2\log(\frac{2}{\delta})}{n}}$, and $\mathcal{A}_\phi(\mathcal{F}, h) = \mathcal{R}_\phi^*(\mathcal{F}, h) - \mathcal{R}_\phi^*(h)$ is the approximation error.

Proof. Excess risk can be decomposed into estimation error and approximation error

$$\mathcal{R}_\phi(r, h) - \mathcal{R}_\phi^*(h) = \underbrace{\mathcal{R}_\phi(r, h) - \mathcal{R}_\phi^*(\mathcal{F}, h)}_{\text{Estimation Error}} + \underbrace{\mathcal{R}_\phi^*(\mathcal{F}, h) - \mathcal{R}_\phi^*(h)}_{\text{Approximation Error}}$$

From Theorem 3.3, we have an upper bound on the estimation error and so using that, we have the following inequality

$$\mathcal{R}_\phi(r, h) - \mathcal{R}_\phi^*(h) \leq \frac{4\rho\sqrt{2(\bar{C}^2 + \bar{l}^2)}}{L} \sum_{j=1}^L \mathfrak{R}_n(\mathcal{F}_j) + (\bar{C} + \bar{l})\sqrt{\frac{2\log\left(\frac{2}{\delta}\right)}{n}} + \mathcal{A}_\phi(\mathcal{F}, h)$$

Since ϕ is binary classification calibrated, we know that

$$\mathcal{R}_{\text{binary } 0-1}(f) - \mathcal{R}_{\text{binary } 0-1}^* \leq \psi^{-1}(\mathcal{R}_{\text{binary } \phi}(f) - \mathcal{R}_{\text{binary } \phi}^*)$$

where ψ is a non-decreasing convex function, making ψ^{-1} a non-decreasing concave function. The proof is complete by using Lemma 3.1 \square

B Proofs for Section 4

B.1 Proof of Lemma B.1

Lemma B.1. *For any $h, r, x \in \mathcal{X}, y \in \mathcal{Y}$, the following equality holds*

$$\mathcal{L}^{\text{OneTime}}(h, r, x, y) = \sum_{j \in \mathcal{J}} (c_{\max} - l(y, \hat{y}_{\leq j}) - \tilde{c}_j(x, \hat{y}_{< j}, y)) \mathbf{1}_{r(x) \neq j} - (|\mathcal{J}| - 1)c_{\max} + \sum_{j \in \mathcal{J}} l(y, \hat{y}_{\leq j}) + \sum_{j \in \mathcal{J}} \tilde{c}_j(x, \hat{y}_{< j}, y)$$

Proof.

$$\begin{aligned} & \mathcal{L}^{\text{OneTime}}(h, r, x, y) \\ &= \sum_{j \in \mathcal{J}} (l(y, \hat{y}_{\leq j}) + \tilde{c}_j(x, \hat{y}_{< j}, y)) \mathbf{1}_{r(x)=j} \\ &= \sum_{j \in \mathcal{J}} (l(y, \hat{y}_{\leq j}) + \tilde{c}_j(x, \hat{y}_{< j}, y)) - \sum_{j \in \mathcal{J}} (l(y, \hat{y}_{\leq j}) + \tilde{c}_j(x, \hat{y}_{< j}, y)) \mathbf{1}_{r(x) \neq j} \\ &= \sum_{j \in \mathcal{J}} (l(y, \hat{y}_{\leq j}) + \tilde{c}_j(x, \hat{y}_{< j}, y)) - \sum_{j \in \mathcal{J}} (l(y, \hat{y}_{\leq j}) + \tilde{c}_j(x, \hat{y}_{< j}, y)) \mathbf{1}_{r(x) \neq j} + (|\mathcal{J}| - 1)c_{\max} - (|\mathcal{J}| - 1)c_{\max} \\ &= \sum_{j \in \mathcal{J}} (l(y, \hat{y}_{\leq j}) + \tilde{c}_j(x, \hat{y}_{< j}, y)) - \sum_{j \in \mathcal{J}} (l(y, \hat{y}_{\leq j}) + \tilde{c}_j(x, \hat{y}_{< j}, y)) \mathbf{1}_{r(x) \neq j} + \sum_{j \in \mathcal{J}} c_{\max} \mathbf{1}_{r(x) \neq j} - (|\mathcal{J}| - 1)c_{\max} \\ &= \sum_{j \in \mathcal{J}} (c_{\max} - l(y, \hat{y}_{\leq j}) - \tilde{c}_j(x, \hat{y}_{< j}, y)) \mathbf{1}_{r(x) \neq j} - (|\mathcal{J}| - 1)c_{\max} + \sum_{j \in \mathcal{J}} l(y, \hat{y}_{\leq j}) + \sum_{j \in \mathcal{J}} \tilde{c}_j(x, \hat{y}_{< j}, y) \end{aligned}$$

\square

B.2 Proof of Proposition B.2

Proposition B.2. $\mathcal{L}^\psi(h, r, x, y)$ is a convex upper bound of $\mathcal{L}^{\text{OneTime}}(h, r, x, y)$ for $\psi \equiv \psi_{ce}$ and $\psi \equiv \psi_{mae}$ upto some scale γ if $c_{\max} > \frac{1}{|\mathcal{J}| - 1} \sum_{j \in \mathcal{J}} (l(y, \hat{y}_{\leq j}) + \tilde{c}_j(x, \hat{y}_{< j}, y))$

Proof. It is easy to see that $\mathcal{L}^\psi(h, r, x, y)$ is convex with respect to r as $\psi_{ce}(\cdot)$ and $\psi_{mae}(\cdot)$ are convex.

From Lemma B.1, we know that

$$\begin{aligned} \mathcal{L}^{\text{OneTime}}(h, r, x, y) &= \sum_{j \in \mathcal{J}} (c_{\max} - l(y, \hat{y}_{\leq j}) - \tilde{c}_j(x, \hat{y}_{< j}, y)) \mathbf{1}_{r(x) \neq j} - (|\mathcal{J}| - 1)c_{\max} + \sum_{j \in \mathcal{J}} l(y, \hat{y}_{\leq j}) + \sum_{j \in \mathcal{J}} \tilde{c}_j(x, \hat{y}_{< j}, y) \\ &\leq \sum_{j \in \mathcal{J}} (c_{\max} - l(y, \hat{y}_{\leq j}) - \tilde{c}_j(x, \hat{y}_{< j}, y)) \mathbf{1}_{r(x) \neq j} \end{aligned}$$

If $r(x) \neq j$, then $\psi_{\text{ce}}(\mathbf{g}(x), j) \geq \log 2$ and $\psi_{\text{mae}}(\mathbf{g}(x), j) \geq 0.5$. When $r(x) = j$, $\psi_{\text{ce}}(\mathbf{g}(x), j) \geq 0$ and $\psi_{\text{mae}}(\mathbf{g}(x), j) \geq 0$. Therefore, $\gamma_{\text{ce}}\psi_{\text{ce}}(\mathbf{g}(x), j) \geq \mathbf{1}_{r(x) \neq j}$ and $\gamma_{\text{mae}}\psi_{\text{mae}}(\mathbf{g}(x), j) \geq \mathbf{1}_{r(x) \neq j}$ where $\gamma_{\text{ce}} = \log 0.5$ and $\gamma_{\text{mae}} = 2$. So then,

$$\begin{aligned} \mathcal{L}^{\text{OneTime}}(h, r, x, y) &\leq \sum_{j \in \mathcal{J}} (c_{\max} - l(y, \hat{y}_{\leq j}) - \tilde{c}_j(x, \hat{y}_{< j}, y)) \mathbf{1}_{r(x) \neq j} \\ &\leq \gamma \sum_{j \in \mathcal{J}} (c_{\max} - l(y, \hat{y}_{\leq j}) - \tilde{c}_j(x, \hat{y}_{< j}, y)) \psi(\mathbf{g}(x), j) \end{aligned}$$

Therefore, $\gamma \mathcal{L}^\psi(h, r, x, y) \geq \mathcal{L}^{\text{OneTime}}(h, r, x, y)$

□

B.3 Proof of Lemma B.3

Lemma B.3. Let $\tilde{c}_j(x, \hat{y}_{< j}, y) \leq \bar{C} < \infty$, $l(y, \hat{y}_j^h) \leq \bar{l} < \infty$ for all $j \in \mathcal{J}$, and ψ be a multiclass surrogate loss that satisfies the following inequality for any distribution over $\mathcal{X} \times \mathcal{J}$ and any measurable function f :

$$\mathcal{R}_{\text{multi } 0-1}(f) - \mathcal{R}_{\text{multi } 0-1}^*(f) \leq \Gamma(\mathcal{R}_{\text{multi } \psi}(f) - \mathcal{R}_{\text{multi } \psi}^*(f))$$

where $\mathcal{R}_{\text{multi } 0-1}$ is the multiclass 0-1 risk and $\Gamma: \mathbb{R}^+ \rightarrow \mathbb{R}^+$ is a non-decreasing concave function. If there exists $i, j \in \mathcal{J}$ such that $|l(y, \hat{y}_i^h) + \tilde{c}_i(x, \hat{y}_{< i}, y) - l(y, \hat{y}_j^h) - \tilde{c}_j(x, \hat{y}_{< j}, y)| > \Delta > 0$, then for any \mathbf{g} over all measurable functions and for any h , the following inequality holds for any distribution over $\mathcal{X} \times \mathcal{Y}$:

$$\mathcal{R}_{\text{OneTime}}(r, h) - \mathcal{R}_{\text{OneTime}}^*(h) \leq \tilde{\Gamma}(\mathcal{R}_\psi(r, h) - \mathcal{R}_\psi^*(h))$$

where $\tilde{\Gamma}(z) = (|\mathcal{J}| - 1)(\bar{C} + \bar{l})\Gamma(\frac{z}{\Delta})$, $\mathcal{R}_{\text{OneTime}}^*(h) = \inf_{r \in \mathcal{M}} \mathcal{R}_{\text{OneTime}}(r, h)$, and $\mathcal{R}_\psi^*(h) = \inf_r \mathcal{R}_\psi(r, h)$

Proof. Let $C_{\text{OneTime}}(r, h, x) = \mathbb{E}_{y \sim \mathcal{P}_{\mathcal{Y}}|X=x} [\mathcal{L}^{\text{OneTime}}(h, r, x, y)]$ be the pointwise $\mathcal{L}^{\text{OneTime}}$ -risk for a given x and predictor h and let $C_{\text{OneTime}}^*(h, x) = \inf_r C_{\text{OneTime}}(r, h, x)$ be the optimal pointwise $\mathcal{L}^{\text{OneTime}}$ -risk for a given x and predictor h . Similarly, let $C_\psi(r, h, x) = \mathbb{E}_{y \sim \mathcal{P}_{\mathcal{Y}}|X=x} [\mathcal{L}_\psi^{\text{OneTime}}(h, r, x, y)]$ be the pointwise \mathcal{L}^ψ -risk for a given x and predictor h and $C_\psi^*(h, x) = \inf_r C_\psi(r, h, x)$ be the optimal pointwise \mathcal{L}^ψ -risk for a given x and predictor h . For any measurable function \mathbf{g}

$$\begin{aligned} &C_{\text{OneTime}}(r, h, x) - C_{\text{OneTime}}^*(h, x) \\ &= \mathbb{E}_{y \sim \mathcal{P}_{\mathcal{Y}}|X=x} \left[\sum_{j \in \mathcal{J}} (l(y, \hat{y}_{\leq j}) + \tilde{c}_j(x, \hat{y}_{< j}, y)) \mathbf{1}_{r(x)=j} \right] \\ &\quad - \inf_{\tilde{r}} \mathbb{E}_{y \sim \mathcal{P}_{\mathcal{Y}}|X=x} \left[\sum_{j \in \mathcal{J}} (l(y, \hat{y}_{\leq j}) + \tilde{c}_j(x, \hat{y}_{< j}, y)) \mathbf{1}_{\tilde{r}(x)=j} \right] \\ &\stackrel{(a)}{=} \mathbb{E}_{y \sim \mathcal{P}_{\mathcal{Y}}|X=x} \left[\sum_{j \in \mathcal{J}} (c_{\max} - l(y, \hat{y}_{\leq j}) - \tilde{c}_j(x, \hat{y}_{< j}, y)) \mathbf{1}_{r(x) \neq j} - (|\mathcal{J}| - 1)c_{\max} + \sum_{j \in \mathcal{J}} l(y, \hat{y}_{\leq j}) + \sum_{j \in \mathcal{J}} \tilde{c}_j(x, \hat{y}_{< j}, y) \right] \\ &\quad - \inf_{\tilde{r}} \mathbb{E}_{y \sim \mathcal{P}_{\mathcal{Y}}|X=x} \left[\sum_{j \in \mathcal{J}} (c_{\max} - l(y, \hat{y}_{\leq j}) - \tilde{c}_j(x, \hat{y}_{< j}, y)) \mathbf{1}_{\tilde{r}(x) \neq j} - (|\mathcal{J}| - 1)c_{\max} + \sum_{j \in \mathcal{J}} l(y, \hat{y}_{\leq j}) + \sum_{j \in \mathcal{J}} \tilde{c}_j(x, \hat{y}_{< j}, y) \right] \\ &= \sum_{j \in \mathcal{J}} \mathbb{E}_{y \sim \mathcal{P}_{\mathcal{Y}}|X=x} [c_{\max} - l(y, \hat{y}_{\leq j}) - \tilde{c}_j(x, \hat{y}_{< j}, y)] \mathbf{1}_{r(x) \neq j} - \inf_{\tilde{r}} \sum_{j \in \mathcal{J}} \mathbb{E}_{y \sim \mathcal{P}_{\mathcal{Y}}|X=x} [c_{\max} - l(y, \hat{y}_{\leq j}) - \tilde{c}_j(x, \hat{y}_{< j}, y)] \mathbf{1}_{\tilde{r}(x) \neq j} \end{aligned}$$

(a) By Lemma B.1. Let $A_j = \mathbb{E}_{y \sim \mathcal{P}_{Y|X=x}} [c_{\max} - l(y, \hat{y}_{\leq j}) - \tilde{c}_j(x, \hat{y}_{< j}, y)]$

$$\begin{aligned} & C_{\text{OneTime}}(r, h, x) - C_{\text{OneTime}}^*(h, x) \\ &= \sum_{j \in \mathcal{J}} A_j \mathbf{1}_{r(x) \neq j} - \inf_{\tilde{r}} \sum_{j \in \mathcal{J}} A_j \mathbf{1}_{\tilde{r}(x) \neq j} \\ &= \sum_{k \in \mathcal{J}} A_k \left(\sum_{j \in \mathcal{J}} \frac{A_j}{\sum_{k \in \mathcal{J}} A_k} \mathbf{1}_{r(x) \neq j} - \inf_{\tilde{r}} \sum_{j \in \mathcal{J}} \frac{A_j}{\sum_{k \in \mathcal{J}} A_k} \mathbf{1}_{\tilde{r}(x) \neq j} \right) \end{aligned}$$

Consider a degenerate distribution on \tilde{X} with a pmf of 1 on x . Let $P(\tilde{Y} = j \mid \tilde{X} = x) = \frac{A_j}{\sum_{k \in \mathcal{J}} A_k}$ and f be a measurable function such that $f(x) = r(x)$. Under this distribution,

$$\begin{aligned} \mathcal{R}_{\text{multi } 0-1}(r) &= \sum_{j \in \mathcal{J}} \frac{A_j}{\sum_{k \in \mathcal{J}} A_k} \mathbf{1}_{r(x) \neq j} & \mathcal{R}_{\text{multi } 0-1}^* &= \inf_{\tilde{r}} \sum_{j \in \mathcal{J}} \frac{A_j}{\sum_{k \in \mathcal{J}} A_k} \mathbf{1}_{\tilde{r}(x) \neq j} \\ \mathcal{R}_{\text{multi } \psi}(r) &= \sum_{j \in \mathcal{J}} \frac{A_j}{\sum_{k \in \mathcal{J}} A_k} \psi(\mathbf{g}(x), j) & \mathcal{R}_{\text{multi } \psi}^* &= \inf_{\tilde{g}} \sum_{j \in \mathcal{J}} \frac{A_j}{\sum_{k \in \mathcal{J}} A_k} \psi(\mathbf{g}(x), j) \end{aligned}$$

From the theorem statement,

$$\begin{aligned} & C_{\text{OneTime}}(r, h, x) - C_{\text{OneTime}}^*(h, x) \\ &= \sum_{k \in \mathcal{J}} A_k \left(\sum_{j \in \mathcal{J}} \frac{A_j}{\sum_{k \in \mathcal{J}} A_k} \mathbf{1}_{r(x) \neq j} - \inf_{\tilde{r}} \sum_{j \in \mathcal{J}} \frac{A_j}{\sum_{k \in \mathcal{J}} A_k} \mathbf{1}_{\tilde{r}(x) \neq j} \right) \\ &\leq \sum_{k \in \mathcal{J}} A_k \Gamma \left(\sum_{j \in \mathcal{J}} \frac{A_j}{\sum_{k \in \mathcal{J}} A_k} \psi(\mathbf{g}(x), j) - \inf_{\tilde{g}} \sum_{j \in \mathcal{J}} \frac{A_j}{\sum_{k \in \mathcal{J}} A_k} \psi(\tilde{\mathbf{g}}(x), j) \right) \end{aligned}$$

We know that $\sum_{j \in \mathcal{J}} A_j \leq (|\mathcal{J}| - 1)(\bar{C} + \bar{l})$ from:

$$\begin{aligned} \sum_{j \in \mathcal{J}} A_j &= \sum_{j \in \mathcal{J}} \mathbb{E}_{y \sim \mathcal{P}_{Y|X=x}} [c_{\max} - l(y, \hat{y}_{\leq j}) - \tilde{c}_j(x, \hat{y}_{< j}, y)] \\ &\leq (|\mathcal{J}| - 1)(\bar{C} + \bar{l}) \end{aligned}$$

Since $l(y, \hat{y}_i^h) + \tilde{c}_i(x, \hat{y}_{< i}, y) \neq l(y, \hat{y}_j^h) + \tilde{c}_i(x, \hat{y}_{< i}, y)$ for a pair (i, j) , we can assume that $\sum_{j \in \mathcal{J}} A_j \geq \Delta$ if $|l(y, \hat{y}_i^h) + \tilde{c}_i(x, \hat{y}_{< i}, y) - l(y, \hat{y}_j^h) - \tilde{c}_i(x, \hat{y}_{< i}, y)| > \Delta$.

With these bounds,

$$\begin{aligned} & C_{\text{OneTime}}(r, h, x) - C_{\text{OneTime}}^*(h, x) \\ &\leq \sum_{k \in \mathcal{J}} A_k \Gamma \left(\sum_{j \in \mathcal{J}} \frac{A_j}{\sum_{k \in \mathcal{J}} A_k} \psi(\mathbf{g}(x), j) - \inf_{\tilde{g}} \sum_{j \in \mathcal{J}} \frac{A_j}{\sum_{k \in \mathcal{J}} A_k} \psi(\tilde{\mathbf{g}}(x), j) \right) \\ &\leq (|\mathcal{J}| - 1)(\bar{C} + \bar{l}) \Gamma \left(\frac{\sum_{j \in \mathcal{J}} A_j \psi(\mathbf{g}(x), j) - \inf_{\tilde{g}} \sum_{j \in \mathcal{J}} A_j \psi(\tilde{\mathbf{g}}(x), j)}{\Delta} \right) \\ &= (|\mathcal{J}| - 1)(\bar{C} + \bar{l}) \Gamma \left(\frac{C_{\psi}(r, h, x) - C_{\psi}^*(h, x)}{\Delta} \right) \end{aligned}$$

Let $\tilde{\Gamma}(z) = (|\mathcal{J}| - 1) (\bar{C} + \bar{l}) \Gamma\left(\frac{z}{\Delta}\right)$. Then,

$$\begin{aligned} \mathcal{R}_{\text{OneTime}}(r, h) - \mathcal{R}_{\text{OneTime}}^*(h) &= \mathbb{E}_{x \sim \mathcal{P}_X} [C_{\text{OneTime}}(r, h, x) - C_{\text{OneTime}}^*(h, x)] \\ &\leq \mathbb{E}_{x \sim \mathcal{P}_X} [\tilde{\Gamma}(C_\psi(r, h, x) - C_\psi^*(h, x))] \\ &\stackrel{(a)}{\leq} \tilde{\Gamma} \left(\mathbb{E}_{x \sim \mathcal{P}_X} [C_\psi(r, h, x) - C_\psi^*(h, x)] \right) \\ &\stackrel{(b)}{=} \tilde{\Gamma}(\mathcal{R}_\psi(r, h) - \mathcal{R}_\psi^*(h)) \end{aligned}$$

(a) by Jensen's inequality since $\tilde{\Gamma}$ is concave, (b) since the infimum is taken over all measurable functions $\mathcal{R}_\psi^*(h) = \mathbb{E}_{x \sim \mathcal{P}_X} [C_\psi^*(h, x)]$ \square

B.4 Proof of Theorem 4.1

Theorem B.4 (Consistency). *Let $\tilde{c}_j(x, \hat{y}_{<j}, y) \leq \bar{C} < \infty$, $l(y, \hat{y}_j^h) \leq \bar{l} < \infty$ for all $j \in \mathcal{J}$, and ψ be cross entropy loss ψ_{ce} or mean absolute error ψ_{mae} . If there exists $i, j \in \mathcal{J}$ such that $|l(y, \hat{y}_i^h) + \tilde{c}_i(x, \hat{y}_{<i}, y) - l(y, \hat{y}_j^h) - \tilde{c}_j(x, \hat{y}_{<j}, y)| > \Delta > 0$, then, for a fixed h , \mathcal{L}^ψ is a consistent surrogate for $\mathcal{L}^{\text{OneTime}}$*

Proof. We know that $\mathcal{R}_{\text{multi } 0-1}(f) - \mathcal{R}_{\text{multi } 0-1}^* \leq \Gamma_{ce}(\mathcal{R}_{\text{multi } \psi_{ce}}(f) - \mathcal{R}_{\text{multi } \psi_{ce}}^*)$ from Theorem 3.1 of Mao et al. (2023) where $\Gamma_{ce}^{-1}(z) = \frac{1+z}{2} \log(1+z) + \frac{1-z}{2} \log(1-z)$. Similarly, $\mathcal{R}_{\text{multi } 0-1}(f) - \mathcal{R}_{\text{multi } 0-1}^* \leq \Gamma_{mae}(\mathcal{R}_{\text{multi } \psi_{mae}}(f) - \mathcal{R}_{\text{multi } \psi_{mae}}^*)$ where $\Gamma_{mae}^{-1}(z) = \frac{z}{L+1}$. Both Γ_{ce}^{-1} and Γ_{mae}^{-1} are non-decreasing convex functions making Γ_{ce} and Γ_{mae} non-decreasing *concave* functions on \mathbb{R}^+ domain.

Let $\Gamma \equiv \Gamma_{ce}$ when $\psi \equiv \psi_{ce}$ and $\Gamma \equiv \Gamma_{mae}$ when $\psi \equiv \psi_{mae}$. By Lemma B.3, $\mathcal{R}_{\text{OneTime}}(r) - \mathcal{R}_{\text{OneTime}}^* \leq \tilde{\Gamma}(\mathcal{R}_\psi(r) - \mathcal{R}_\psi^*)$ where $\tilde{\Gamma}(z) = (|\mathcal{J}| - 1) (\bar{C} + \bar{l}) \Gamma\left(\frac{z}{\Delta}\right)$. If $\lim_{n \rightarrow \infty} \mathcal{R}_\psi(r_n) - \mathcal{R}_\psi^* = 0$, then

$$\begin{aligned} \lim_{n \rightarrow \infty} \mathcal{R}_{\text{Point}}(r_n) - \mathcal{R}_{\text{Point}}^* &\leq \lim_{n \rightarrow \infty} \tilde{\Gamma}(\mathcal{R}_\psi(r_n) - \mathcal{R}_\psi^*) \\ &\stackrel{(a)}{=} (|\mathcal{J}| - 1) (\bar{C} + \bar{l}) \Gamma \left(\lim_{n \rightarrow \infty} \frac{\mathcal{R}_\psi(r_n) - \mathcal{R}_\psi^*}{\Delta} \right) \\ &= (|\mathcal{J}| - 1) (\bar{C} + \bar{l}) \Gamma(0) \\ &\stackrel{(b)}{=} 0 \end{aligned}$$

(a) by continuity of Γ at 0 and (b) since $\Gamma_{ce}(0) = 0$ and $\Gamma_{mae}(0) = 0$ \square

B.5 Proof of Theorem 4.2

Theorem B.5. *Suppose $r_n \in \mathcal{F} = \{x \rightarrow \arg \min_{j \in \mathcal{J}} g_j(x) : g_j \in \mathcal{G}_j\}$ where \mathcal{G}_j consists of functions having a range of $(-M, M)$ with $M \geq 0$, $\tilde{c}_j(x, \hat{y}_{<j}, y) \leq \bar{C}$, and $l(y, \hat{y}_j^h) \leq \bar{l} < \infty$. If ψ is ρ -lipschitz continuous with respect to $\mathbf{g}(x)$ and there exists $u_\psi(M)$ such that $\psi(\mathbf{g}(x), j) \leq u_\psi(M) < \infty$ for all $j \in \mathcal{J}$ and $r \in \mathcal{F}$, then with probability $1 - \delta$ for a fixed h , the following upper bound holds for the empirical risk minimizer \hat{r}_n with respect to \mathcal{L}^ψ :*

$$\mathcal{R}_\psi(\hat{r}_n, h) - \mathcal{R}_\psi^*(\mathcal{F}, h) \leq 2\sqrt{2}q(L)\rho \sum_{j \in \mathcal{J}} \mathfrak{R}_n(\mathcal{G}_j) + u_\psi(M)q(L) \sqrt{\frac{2 \log(\frac{2}{\delta})}{n}}$$

where $\mathcal{R}_\psi^*(\mathcal{F}, h) = \inf_{r \in \mathcal{F}} \mathcal{R}_\psi(r, h)$, $q(L) = 2(|\mathcal{J}| - 1)(\bar{C} + \bar{l})$, and $\mathfrak{R}_n(\mathcal{G}_j)$ is the Rademacher Complexity of \mathcal{G}_j .

Proof. Let $G_n = \sup_{r \in \mathcal{F}} [\mathcal{R}_\psi(r) - \widehat{\mathcal{R}}_\psi(r)]$, $G_{n'} = \sup_{r \in \mathcal{F}} [\widehat{\mathcal{R}}_\psi(r) - \mathcal{R}_\psi(r)]$, and $\mathcal{B} = \{(x, y) \mapsto \mathcal{L}^\psi(h, r, x, y) : r \in \mathcal{F}\}$.

If $z^i = (x^i, y^i)$, $G_n = g(z^1, \dots, z^n)$.

$$\begin{aligned} \left| g(z^1, \dots, z^i, \dots, z^n) - g(z^1, \dots, z^{i'}, \dots, z^n) \right| &\leq \frac{1}{n_c} \left| \sup_{r \in \mathcal{F}} \mathcal{L}^\psi(h, r, x^i, y^i) - \mathcal{L}^\psi(h, r, x^{i'}, y^{i'}) \right| \\ &\leq \frac{1}{n} \sup_{r \in \mathcal{F}} \sum_{j \in \mathcal{J}} \left| (c_{\max}^i - l(y^i, \widehat{y}_{\leq j}^i) - \tilde{c}_j(x^i, \widehat{y}_{< j}^i, y^i)) \psi(\mathbf{g}(x^i), y^i) \right| \\ &\quad + \left| (c_{\max}^{i'} - l(y^{i'}, \widehat{y}_{\leq j}^{i'}) - \tilde{c}_j(x^{i'}, \widehat{y}_{< j}^{i'}, y^{i'})) \psi(\mathbf{g}(x^{i'}), y^{i'}) \right| \\ &\leq \frac{1}{n} u_\psi(M) 2(|\mathcal{J}| - 1)(\bar{C} + \bar{l}) \\ &= \frac{1}{n} u_\psi(M) q(L) \end{aligned}$$

where $q(L) = 2(|\mathcal{J}| - 1)(\bar{C} + \bar{l})$. Using this boundedness property, we can apply McDiarmid's inequality

$$\begin{aligned} P\left(G_n > \frac{\epsilon}{2}\right) &\leq \exp\left\{ \frac{-2\left(\frac{\epsilon}{2} - \mathbb{E}[G_n]\right)^2}{\sum_{i=1}^{n_c} \frac{u_\psi(M)^2 q(L)^2}{n^2}} \right\} \\ &\leq \exp\left\{ \frac{-2n\left(\frac{\epsilon}{2} - 2\mathfrak{R}_n(\mathcal{B})\right)^2}{u_\psi(M)^2 q(L)^2} \right\} \\ &\stackrel{\text{def}}{=} \frac{\delta}{2} \end{aligned}$$

Similarly,

$$P\left(G_{n'} > \frac{\epsilon}{2}\right) \leq \exp\left\{ \frac{-2n\left(\frac{\epsilon}{2} - 2\mathfrak{R}_n(\mathcal{B})\right)^2}{u_\psi(M)^2 q(L)^2} \right\} = \frac{\delta}{2}$$

Then $\epsilon = 4\mathfrak{R}_n(\mathcal{B}) + u_\psi(M)q(L)\sqrt{\frac{2\log(\frac{2}{\delta})}{n}}$

$$\begin{aligned} P\left(\mathcal{R}_\psi(\widehat{r}_n) - \mathcal{R}_\psi^*(\mathcal{F}) > \epsilon\right) &\leq P\left(\sup_{r \in \mathcal{F}} \left| \mathcal{R}_\psi(r) - \widehat{\mathcal{R}}_\psi(r) \right| > \frac{\epsilon}{2}\right) \\ &\leq P\left(G_n > \frac{\epsilon}{2}\right) + P\left(G_{n'} > \frac{\epsilon}{2}\right) \\ &\leq \delta \end{aligned}$$

With at least probability $1 - \delta$, $\mathcal{R}_\psi(\widehat{r}_n, h) - \mathcal{R}_\psi^*(\mathcal{F}, h) \leq 4\mathfrak{R}_n(\mathcal{B}) + u_\psi(M)q(L)\sqrt{\frac{2\log(\frac{2}{\delta})}{n}}$.

We can further bound $\mathfrak{R}_n(\mathcal{B})$ by $\mathfrak{R}_n(\mathcal{F}_j)$ if we show that \mathcal{L}^ψ is Lipschitz continuous with respect to \mathbf{g}

$$\begin{aligned}
& \|\mathcal{L}^\psi(h, r^1, x, y) - \mathcal{L}^\psi(h, r^2, x, y)\|_2 \\
&= \left\| \sum_{j \in \mathcal{J}} (c_{\max} - l(y, \hat{y}_{\leq j}) - \tilde{c}_j(x, \hat{y}_{< j}, y)) \psi(\mathbf{g}^1(x), j) - \sum_{j \in \mathcal{J}} (c_{\max} - l(y, \hat{y}_{\leq j}) - \tilde{c}_j(x, \hat{y}_{< j}, y)) \psi(\mathbf{g}^2(x), j) \right\|_2 \\
&\leq \sum_{j \in \mathcal{J}} (c_{\max} - l(y, \hat{y}_{\leq j}) - \tilde{c}_j(x, \hat{y}_{< j}, y)) \|\psi(\mathbf{g}^1(x), j) - \psi(\mathbf{g}^2(x), j)\|_2 \\
&\stackrel{(a)}{=} \sum_{j \in \mathcal{J}, j \neq j_{\max}} (c_{\max} - l(y, \hat{y}_{\leq j}) - \tilde{c}_j(x, \hat{y}_{< j}, y)) \|\psi(\mathbf{g}^1(x), j) - \psi(\mathbf{g}^2(x), j)\|_2 \\
&\stackrel{(b)}{\leq} \sum_{j \in \mathcal{J}, j \neq j_{\max}} (\bar{C} + \bar{l}) \rho \|\mathbf{g}^1(x) - \mathbf{g}^2(x)\|_2 \\
&= (\mathcal{J} - 1) (\bar{C} + \bar{l}) \rho \|\mathbf{g}^1(x) - \mathbf{g}^2(x)\|_2
\end{aligned}$$

(a) where $j_{\max} = \arg \max_{j \in \mathcal{J}} l(y, \hat{y}_{\leq j}) + \tilde{c}_j(x, \hat{y}_{< j}, y)$, (b) by lipschitz continuity of ψ .

By the extension of the Talagrand's Contraction Lemma Maurer (2016),

$$\begin{aligned}
\mathfrak{R}_n(\mathcal{B}) &= \mathbb{E}_{\sigma_1, \dots, \sigma_n, \{z^i\}_{i=1}^n \sim \mathcal{P}_{\mathcal{X} \times \mathcal{Y}}} \left[\sup_{b \in \mathcal{B}} \frac{1}{n} \sum_{i=1}^n \sigma_i b(z^i) \right] \\
&\leq (|\mathcal{J}| - 1) (\bar{C} + \bar{l}) \rho \sqrt{2} \mathbb{E}_{\sigma, \{z^i\}_{i=1}^n \sim \mathcal{P}_{\mathcal{X} \times \mathcal{Y}}} \left[\sup_{\mathbf{g} \in \mathcal{G}_1 \times \dots \times \mathcal{G}_{L+1}} \frac{1}{n} \sum_{i=1}^n \sum_{j \in \mathcal{J}} \sigma_{i,j} g_j(z^i) \right] \\
&\leq \frac{q(L)\rho}{\sqrt{2}} \sum_{j \in \mathcal{J}} \mathbb{E}_{\sigma, \{z^i\}_{i=1}^n \sim \mathcal{P}_{\mathcal{X} \times \mathcal{Y}}} \left[\sup_{g_j \in \mathcal{G}_j} \frac{1}{n} \sum_{i=1}^n \sigma_{i,j} g_j(z^i) \right] \\
&\leq \frac{q(L)\rho}{\sqrt{2}} \sum_{j \in \mathcal{J}} \mathfrak{R}_n(\mathcal{G}_j)
\end{aligned}$$

□

B.6 Proof of Corollary B.6

Corollary B.6. *Suppose $r_n \in \mathcal{F} = \{x \rightarrow \arg \min_{j \in \mathcal{J}} g_j(x) : g_j \in \mathcal{G}_j\}$ where \mathcal{G}_j consists of functions having a range of $(-M, M)$ with $M \geq 0$, $\tilde{c}_j(x, \hat{y}_{< j}, y) \leq \bar{C}$, and $l(y, \hat{y}_j^n) \leq \bar{l} < \infty$. If ψ is ψ_{ce} or ψ_{mae} , then with probability $1 - \delta$, for a fixed h , the excess risk of with respect to $\mathcal{L}^{OneTime}$ holds for the empirical risk minimizer \hat{r}_n with respect to \mathcal{L}^ψ*

$$\mathcal{R}_{OneTime}(\hat{r}_n, h) - \mathcal{R}_{OneTime}^*(h) \leq \tilde{\Gamma} \left(2q(L)\rho\sqrt{2} \sum_{j \in \mathcal{J}} \mathfrak{R}_n(\mathcal{G}_j) + u_\psi(M)q(L) \sqrt{\frac{2 \log(\frac{2}{\delta})}{n}} + \mathcal{A}_\psi(\mathcal{F}, h) \right)$$

where $\tilde{\Gamma} : \mathbb{R}^+ \rightarrow \mathbb{R}^+$, $q(L) = 2(|\mathcal{J}| - 1)(\bar{C} + \bar{l})$, ρ is the lipschitz norm of ψ , and $\mathcal{A}_\psi(\mathcal{F}, h) = \mathcal{R}_\psi^*(\mathcal{F}, h) - \mathcal{R}_\psi^*(h)$ is the approximation error.

Proof. Excess risk can be decomposed into estimation error and approximation error

$$\mathcal{R}_\psi(r, h) - \mathcal{R}_\psi^*(h) = \underbrace{\mathcal{R}_\psi(r, h) - \mathcal{R}_\psi^*(h)(\mathcal{F}, h)}_{\text{Estimation Error}} + \underbrace{\mathcal{R}_\psi^*(\mathcal{F}, h) - \mathcal{R}_\psi^*(h)}_{\text{Approximation Error}}$$

We know that ψ_{ce}, ψ_{mae} are upper bounded by $u_{\psi_{ce}}(M), u_{\psi_{mae}}(M)$ respectively. We also know that the lipschitz norm for ψ_{ce} ρ_{ce} is $\sqrt{2}$ and the lipschitz norm for ψ_{mae} ρ_{mae} is 2

From Theorem 4.2, we have an upper bound on the estimation error and so using that, we have the following inequality

$$\mathcal{R}_\psi(r, h) - \mathcal{R}_\psi^*(h) \leq 2q(L)\rho\sqrt{2} \sum_{j \in \mathcal{J}} \mathfrak{R}_n(\mathcal{G}_j) + u_\psi(M)q(L) \sqrt{\frac{2 \log(\frac{2}{\delta})}{n}} + \mathcal{A}_\psi(\mathcal{F}, h)$$

$\mathcal{R}_{\text{multi } 0-1}(f) - \mathcal{R}_{\text{multi } 0-1}^*$ $\leq \Gamma_{\text{ce}} \left(\mathcal{R}_{\text{multi } \psi_{\text{ce}}}(f) - \mathcal{R}_{\text{multi } \psi_{\text{ce}}}^* \right)$ from Theorem 3.1 of Mao et al. (2023) where $\Gamma_{\text{ce}}^{-1}(z) = \frac{1+z}{2} \log(1+z) + \frac{1-z}{2} \log(1-z)$. Similarly, $\mathcal{R}_{\text{multi } 0-1}(f) - \mathcal{R}_{\text{multi } 0-1}^* \leq \Gamma_{\text{mae}} \left(\mathcal{R}_{\text{multi } \psi_{\text{mae}}}(f) - \mathcal{R}_{\text{multi } \psi_{\text{mae}}}^* \right)$ where $\Gamma_{\text{mae}}^{-1}(z) = \frac{z}{L+1}$. Both Γ_{ce}^{-1} and Γ_{mae}^{-1} are non-decreasing convex functions making Γ_{ce} and Γ_{mae} non-decreasing *concave* functions on \mathbb{R}^+ domain.

The proof is complete by using Lemma B.3

□

C Baseline Details

For XSUM and TSP, let $p_h(\hat{y}_j | \hat{y}_{<j}, x)$ be the predictive distribution of the j^{th} token conditioned on the leftward context $\hat{y}_{<j}$ and input x . The confidence measure would then be $-\log p_h(\hat{y}_j | \hat{y}_{<j}, x)$ and the predictive entropy would be $H(\hat{Y}_j | \hat{y}_{<j}, x) = -\sum_{v \in \mathcal{V}} p_h(v | \hat{y}_{<j}, x) \log p_h(v | \hat{y}_{<j}, x)$. For MWP, if we assume that there are dropout layers in the predictor network, we can use the Monte Carlo Variance Gal & Ghahramani (2016) or $\text{Var}_h(v | y_{<j}, x)$ across T inference passes as a confidence measure.

For a given threshold τ , the whole deferral decision rule is determined by evaluating $r(x) > \tau$. The baselines offer various ways of modeling r .

- **ChowSum** - For TSP and XSUM, $r_{\text{ChowSum}}(x) = -\sum_{j=1}^L \log p_h(\hat{y}_j | \hat{y}_{<j}, x)$ and for MWP, $r_{\text{ChowSum}}(x) = \sum_{j=1}^L \text{Var}_h(v | y_{<j}, x)$
- **ChowMean** - For TSP and XSUM, $r_{\text{ChowMean}}(x) = -\frac{1}{L} \sum_{j=1}^L \log p_h(\hat{y}_j | \hat{y}_{<j}, x)$ and for MWP, $r_{\text{ChowSum}}(x) = \frac{1}{L} \sum_{j=1}^L \text{Var}_h(v | y_{<j}, x)$
- **ChowQuantile** at the level α - For TSP and XSUM, $r_{\text{ChowQuantile}}^\alpha(x) = \text{Quantile}_\alpha \left(\{-\log p_h(\hat{y}_j | \hat{y}_{<j}, x)\}_{j=1}^L \right)$ and for MWP, $r_{\text{ChowSum}}(x) = \text{Quantile}_\alpha \left(\{\text{Var}_h(v | y_{<j}, x)\}_{j=1}^L \right)$
- **WholeModelEmbed** - $r(x)$ is trained just like **WholeModelScore** but the inputs for the rejector are the inputs to the predictor along with the confidence scores.

Similarly, for token-wise deferral, if $r_j(x, \hat{y}_{<j})$ exceeds threshold τ , the expert is called to predict the next token. r_j can be modeling in the following ways:

- **TokenwiseScore**: For TSP and XSUM, $r_j^{\text{score}}(x, \hat{y}_{<j}) = -\log p_h(\hat{y}_j | \hat{y}_{<j}, x)$ and for MSP, $r_j^{\text{softmax}}(x, \hat{y}_{<j}) = \text{Var}_h(v | y_{<j}, x)$
- **TokenwiseEntropy**: $r_j^{\text{entropy}}(x, \hat{y}_{<j}) = H(\hat{Y}_j | \hat{y}_{<j}, x)$. This only applies to XSUM and TSP.

Since $r(x) = \arg \max_{j \in [1, L+1]} g_j(x)$ for one-time deferral, we consider the following the scoring functions g_j :

- **OneTimeScore**: For TSP and XSUM, $g_j^{\text{score}}(x) = -\log p_h(\hat{y}_j | \hat{y}_{<j}, x)$ and for MSP, $g_j^{\text{score}}(x) = \text{Var}_h(v | y_{<j}, x)$
- **OneTimeEntropy**: $g_j^{\text{entropy}}(x, \hat{y}_{<j}) = H(\hat{Y}_j | \hat{y}_{<j}, x)$. This only applies to XSUM and TSP.

D Training Details and Hyperparameters

All the models were implemented using PyTorch and all the models were trained on an Nvidia A40 GPU. They were trained using Early stopping and Table 2 contains all hyperparameter details.

Task/Hyperparameters	TSP-OneTime	XSUM-Tokenlevel	XSUM-OneTime	MWP-Tokenlevel	MWP-OneTime
Learning rate	5e-4	1e-3	5e-4	5e-4	5e-4
Early Stopping (patience, delta)	20, 1e-4	7, 1e-4	20, 1e-4	7, 1e-4	20, 1e-4
Architecture	MLP	LSTM	MLP	LSTM	MLP
Hidden layers	1	3	1	2	1
Hidden units	8	128	8	64	8
Dropout	0.2	0.4	0.2	0.4	0.2
Epochs	200	100	200	100	200
Training Samples	2400	800	2400	70080	70080
Gradient Clipping Norm	1.0	1.0	1.0	1.0	1.0
Weight Decay	0.005	0.001	0.005	0.001	0.005

Table 2: Hyperparameter settings

TSP: Using the RL4CO library Berto et al. (2023), TSP graphs with 50 nodes were generated by sampling the node coordinates from a standard normal distribution. These samples were fed into a PointerNet (predictor) trained with 10000 samples. The node embeddings, graph context, and log scores from the PointerNet served as inputs for the One-Time rejector. This rejector only took a maximum of 10 minutes to train.

XSUM: During training and inference, Tokenlevel rejector was only exposed to samples with summaries of less than 15 words. The model was trained without teacher forcing. It took about 5 hours to train. The token level rejector r receives the encoder hidden states from the predictor as hidden states and the decoder hidden states as input. This continues in an autoregressive fashion. We defer the reader to Appendix H for ablation studies on various training strategies for the tokenlevel rejector.

The OneTime rejector was trained on a dataset with summaries containing upto 20 words and it took a couple of minutes to train after a dataset of all the varying mixtures of predictions was created (this took a couple of hours to make). This rejector takes the encoder hidden states, decoder hidden states, and log scores from the predictor as input.

MWP: The token-level rejector took about 5 hour to train. e token level rejector r receives the encoder hidden states from the predictor as hidden states and the decoder hidden states as input. This continues in an autoregressive fashion. The OneTime rejector was trained on a dataset containing all the varying mixtures of predictions which took a couple of minutes to generate. This rejector takes the encoder hidden states, decoder hidden states, and monte carlo variance estimates from the predictor as input.

E More Cost-Loss Plots

See Figure 3

F Effects of α_j

In experiments, we determine the cost of deferring a complete prediction and call it α_1 . Then, we set $\alpha_j = \frac{L-j+1}{L}\alpha_1$, making the cost of deferring a token $\frac{\alpha_1}{L}$ or α_L . We vary α_1 and Figure 4 shows how the costs affect cost-accuracy tradeoffs. For both experiments, extreme values for cost often result in poor cost-accuracy tradeoff. For TSP, the results are best when $\alpha_L = 0.01$ and for XSUM, it is either $\alpha_L = 0.01$ or $\alpha_L = 0.015$.

As a general rule of thumb, we propose that α_1 should be determined by the median difference between the expert accuracy and predictor accuracy on the train set.

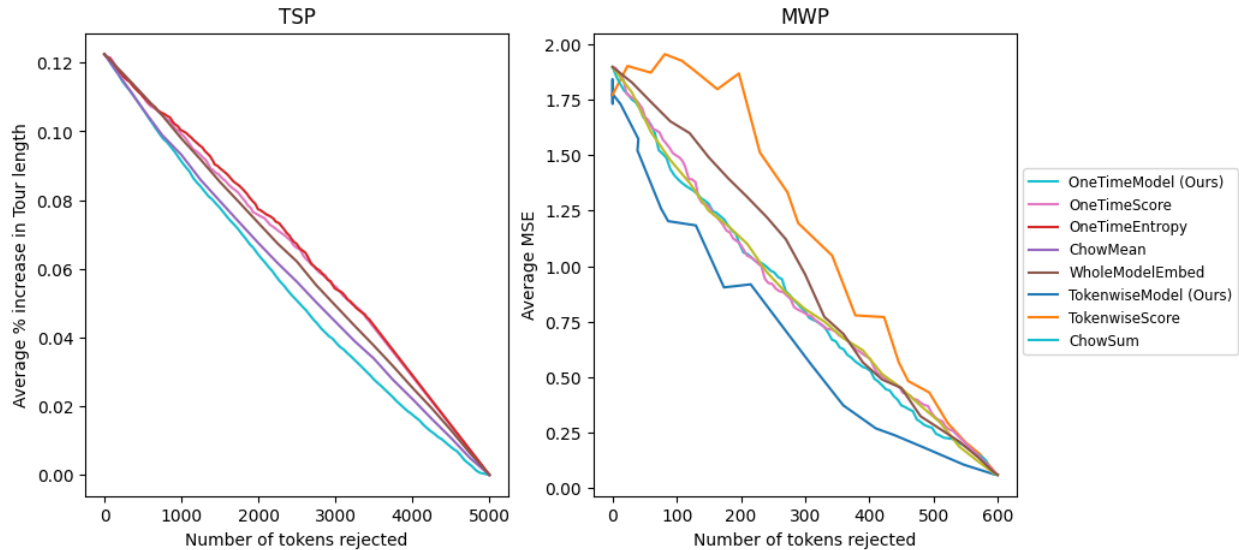


Figure 3: Cost-Loss plots for TSP (on the left) and MWP (on the right).

Size of \mathcal{J}	OneTimeModel (Ours)		OneTimeSoftmax		OneTimeEntropy	
	AUDC	% Improvement	AUDC	% Improvement	AUDC	% Improvement
5	287.37(7.67)	6.13(1.68)	322.08(18.24)	-5.19(4.99)	316.76(19.90)	-3.43(5.30)
10	277.44(10.59)	9.38(2.54)	318.00(12.62)	-3.86(2.95)	317.84(22.77)	-3.78(6.42)
15	277.62(9.15)	9.32(1.85)	320.45(6.89)	-4.68(1.32)	317.87(12.57)	-3.83(3.22)
20	273.34(11.13)	10.74(2.34)	321.35(19.06)	-4.96(5.43)	320.54(22.24)	-4.70(6.68)
25	273.31(12.20)	10.73(3.11)	318.49(12.65)	-4.03(3.18)	321.32(13.95)	-4.97(4.10)
30	271.10(9.77)	11.45(2.16)	319.61(10.82)	-4.39(1.99)	321.67(14.16)	-5.05(3.11)
35	273.30(6.76)	10.72(1.69)	316.40(15.66)	-3.36(4.55)	320.51(20.33)	-4.70(6.20)
40	272.57(10.08)	10.97(2.53)	318.99(14.07)	-4.18(3.49)	320.91(15.41)	-4.82(4.16)
45	270.92(10.67)	11.52(2.41)	318.52(14.10)	-4.04(3.71)	322.02(14.99)	-5.19(4.31)
51	272.64(9.11)	10.95(2.06)	318.96(14.78)	-4.17(3.66)	322.91(14.05)	-5.50(4.39)

Table 3: AUDC scores and Percent improvement over the random baseline in TSP of various sizes of \mathcal{J} with standard deviations in brackets

G AUDC and Percent Improvement for Size of \mathcal{J} experiment

In support of Figure 2, Table 4 and Table 3 report the actual values of AUDC and percent improvement in AUDC over the random baseline for each size of \mathcal{J} considered for both TSP and XSUM.

H Token-level Rejector Ablation

$\mathcal{L}^{\text{Token}}$ bears resemblance to a weighted multi-label classification loss function. Specifically, the token-level rejector follows a classifier chain approach Read et al. (2021). Classifier chains is a multi-label classification (MLC) approach that involves training L binary classifiers in a pre-specified order with the j^{th} binary classifier taking the feature vector and the previous $j - 1$ labels as input, forming a chain of predictors. At inference time, the test features are fed into the chain such that the previous label predictions are appended to the features for the next label classifier. Our token-level rejector r_j implicitly makes these chained predictions by taking in $\hat{y}_{<j}$ which is informed by the previous $(j - 1)$ rejectors' rejection decision.

With this comparison established, model architectures and training techniques from classifier chain literature can be utilized. Recurrent classifier chains Nam et al. (2017) have emerged as a popular choice for MLC

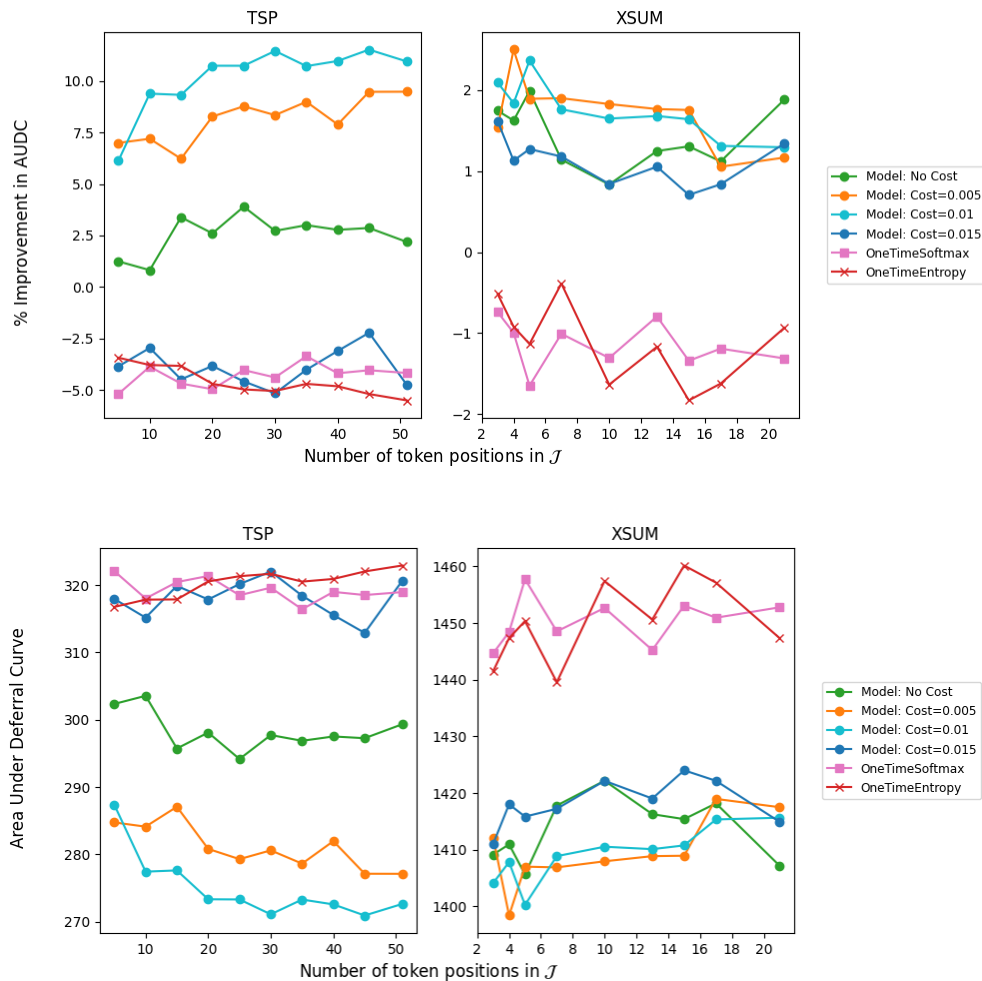


Figure 4: Plots of Size of \mathcal{J} against AUDC and percentage improvement in AUDC relative to the random baseline for TSP (on the left) and XSUM (on the right) for models trained with different α_1 value. The costs displayed in the legend refer to the deferral cost per token or α_L

Size of \mathcal{J}	OneTimeModel (Ours)		OneTimeSoftmax		OneTimeEntropy	
	AUDC	% Improvement	AUDC	% Improvement	AUDC	% Improvement
3	1412.16(26.70)	1.54(0.88)	1444.68(16.16)	-0.74(0.77)	1441.52(18.29)	-0.52(0.61)
4	1398.39(25.51)	2.50(0.80)	1448.43(23.88)	-1.00(0.91)	1447.35(24.59)	-0.92(1.02)
5	1407.01(19.33)	1.89(0.43)	1457.76(23.95)	-1.65(1.11)	1450.36(22.32)	-1.13(1.04)
7	1406.88(19.64)	1.90(0.79)	1448.54(20.05)	-1.01(0.97)	1439.58(16.68)	-0.39(1.20)
10	1407.96(19.47)	1.83(0.34)	1452.68(15.51)	-1.31(1.44)	1457.43(15.44)	-1.63(1.29)
13	1408.87(23.47)	1.76(0.71)	1445.25(12.84)	-0.80(1.78)	1450.64(14.74)	-1.17(1.72)
15	1408.94(16.75)	1.75(0.68)	1453.11(6.66)	-1.34(1.46)	1460.17(14.20)	-1.83(1.43)
17	1418.97(16.00)	1.05(0.59)	1450.95(11.65)	-1.19(1.63)	1457.15(10.29)	-1.62(1.52)
21	1417.50(26.37)	1.17(0.68)	1452.79(15.86)	-1.31(1.30)	1447.35(12.72)	-0.93(1.20)

Table 4: AUDC scores and Percent improvement over the random baseline in XSUM of various sizes of \mathcal{J} with standard deviations in brackets

as they efficiently maximize accuracy without requiring the large number of trainable parameters typically needed for K separate binary classifiers.

Since the inputs of recurrent classifier chains at training time are typically ground truth labels, training token-level rejectors would similarly require using the correct rejection decision, $\mathbf{1}_{l(y, \hat{y}_j^h) > c_j(x, \hat{y}_{<j}, y)}$, to determine the j^{th} token prediction for the next label rejector. Following this strategy, also called “teacher forcing” Williams & Zipser (1989), can often cause a distribution shift, as label predictions will be used at test time instead of the correct label, resulting in errors propagating through the chain. Scheduled sampling Bengio et al. (2015) offers a middle ground by labeling the training data with the correct rejection decision with probability p , and otherwise using the predicted one. This probability p often decays at a linear or exponential rate over epochs, gradually reducing the model’s dependence on ground-truth rejection rules.

We use both Multi Layer Perceptrons (MLP) and Long Short-term memory (LSTM) models to perform token-level deferrals on XSUM data. All models are trained with teacher forcing, without teacher forcing, or with scheduled sampling. The Scheduled sampler decayed the teacher forcing probability exponentially by 0.95 with every epoch and the decay process stopped when the teacher forcing probability was 0.5. The sampler has 5 warmup epochs where the teacher forcing probability was 1.0 before the decay started. The coin flip of whether or not to teacher force occurred on a token-level, as opposed to a batch-level. Figure 5 shows the superiority of recurrent models like LSTMs over MLPs with teacher forcing adversely affecting their performance. The selected model is an LSTM trained without teacher forcing. We present the AUDC scores for each of the models in Table 5.

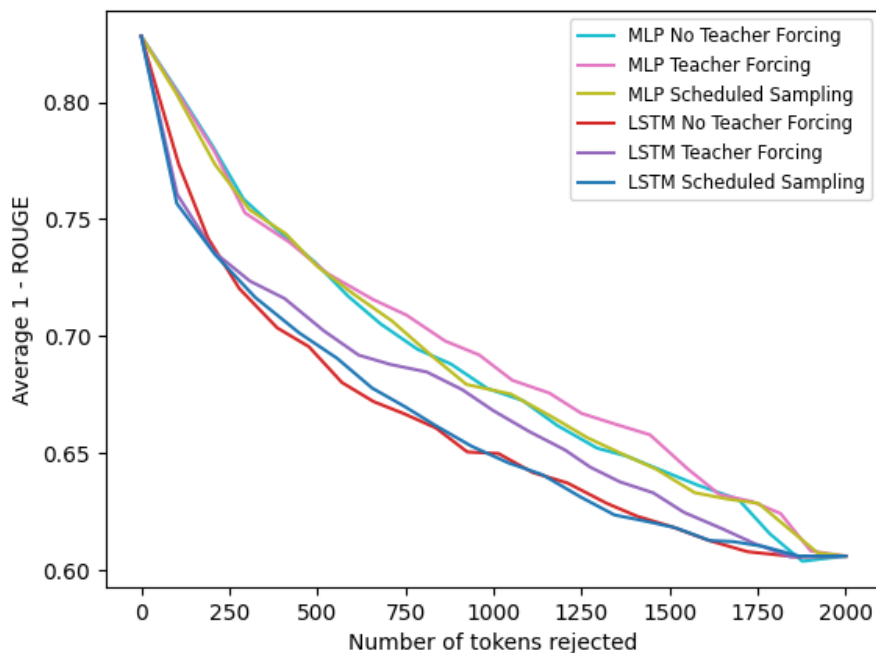


Figure 5: Cost-Loss plots for XSUM for various model architectures and training strategies.

Method	AUC Score	% Improvement
MLP No Teacher Forcing	1375.48 (34.57)	4.07 (1.01)
MLP Teacher Forcing	1387.49 (25.96)	3.22 (1.25)
MLP Scheduled Sampling	1377.01 (31.92)	3.96 (1.20)
LSTM No Teacher Forcing	1323.92 (25.34)	7.66 (0.96)
LSTM Teacher Forcing	1340.43 (20.24)	6.49 (1.24)
LSTM Scheduled Sampling	1324.83 (27.04)	7.60 (0.98)
TokenwiseSoftmax	1354.78 (31.87)	5.51 (0.94)
TokenwiseEntropy	1360.41 (31.50)	5.12 (0.62)

Table 5: AUC Scores for various Token-level Rejector architectures and training